**Atmospheric
Chemistry
and Physics**

A 60 yr record of atmospheric carbon monoxide reconstructed from Greenland firn air

V. V. Petrenko[1,2]**, P. Martinerie**[3]**, P. Novelli**[4]**, D. M. Etheridge**[5]**, I. Levin**[6]**, Z. Wang**[7]**, T. Blunier**[8]**, J. Chappellaz**[3]**,
J. Kaiser**[9]**, P. Lang**[4]**, L. P. Steele**[5]**, S. Hammer**[6]**, J. Mak**[7]**, R. L. Langenfelds**[5]**, J. Schwander**[10]**, J. P. Severinghaus**[11]**,
E. Witrant**[12]**, G. Petron**[4]**, M. O. Battle**[13]**, G. Forster**[9]**, W. T. Sturges**[9]**, J.-F. Lamarque**[14]**, K. Steffen**[15,16]**, and
J. W. C. White**[1,17]

[1]Institute of Arctic and Alpine Research (INSTAAR), University of Colorado, Boulder, CO 80309, USA
[2]Department of Earth and Environmental Sciences, University of Rochester, Rochester, NY 14627, USA
[3]UJF – Grenoble 1/CNRS, Laboratoire de Glaciologie et Géophysique de l'Environnement (LGGE) UMR5183, Grenoble,
38041, France
[4]NOAA ESRL Global Monitoring Division, Boulder, CO 80305, USA
[5]Centre for Australian Weather and Climate Research, CSIRO Marine and Atmospheric Research, Aspendale, Victoria 3195,
Australia
[6]Institut für Umweltphysik, Heidelberg University, 69120 Heidelberg, Germany
[7]School of Marine and Atmospheric Sciences/Institute for Terrestrial and Planetary Atmospheres, State University of New
York at Stony Brook, Stony Brook, NY 11794, USA
[8]Centre for Ice and Climate, Niels Bohr Institute, University of Copenhagen, 2100 København Ø, Denmark
[9]School of Environmental Sciences, University of East Anglia (UEA), Norwich NR4 7TJ, UK
[10]University of Berne, Physics Institute, 3012 Bern, Switzerland
[11]Scripps Institution of Oceanography, University of California, San Diego, La Jolla, CA 92093, USA
[12]UJF – Grenoble 1/CNRS, Grenoble Image Parole Signal Automatique (GIPSA-lab), UMR5216, B.P. 46, 38402 St Martin
d'Hères, France
[13]Department of Physics and Astronomy, Bowdoin College, 8800 College Station, Brunswick, ME 04011, USA
[14]National Center for Atmospheric Research, Boulder, CO 80301, USA
[15]Cooperative Institute for Research in Environmental Sciences, University of Colorado, Boulder, CO 80309, USA
[16]Swiss Federal Research Institute WSL, 8903 Birmensdorf, Switzerland
[17]Geological Sciences and Environmental Studies, University of Colorado, Boulder, CO 80309, USA

Correspondence to: V. V. Petrenko (vpetrenk@z.rochester.edu)

Abstract. We present the first reconstruction of the Northern Hemisphere (NH) high latitude atmospheric carbon monoxide (CO) mole fraction from Greenland firn air. Firn air samples were collected at three deep ice core sites in Greenland (NGRIP in 2001, Summit in 2006 and NEEM in 2008). CO records from the three sites agree well with each other as well as with recent atmospheric measurements, indicating that CO is well preserved in the firn at these sites. CO atmospheric history was reconstructed back to the year 1950 from the measurements using a combination of two forward

models of gas transport in firn and an inverse model. The reconstructed history suggests that Arctic CO in 1950 was 140–150 nmol mol^{-1}, which is higher than today's values. CO mole fractions rose by 10–15 nmol mol^{-1} from 1950 to the 1970s and peaked in the 1970s or early 1980s, followed by a ≈ 30 nmol mol^{-1} decline to today's levels. We compare the CO history with the atmospheric histories of methane, light hydrocarbons, molecular hydrogen, CO stable isotopes and hydroxyl radicals (OH), as well as with published CO emission inventories and results of a historical run from a

chemistry-transport model. We find that the reconstructed Greenland CO history cannot be reconciled with available emission inventories unless unrealistically large changes in OH are assumed. We argue that the available CO emission inventories strongly underestimate historical NH emissions, and fail to capture the emission decline starting in the late 1970s, which was most likely due to reduced emissions from road transportation in North America and Europe.

1 Introduction

Carbon monoxide (CO) is a reactive trace gas that plays a key role in global atmospheric chemistry by being a major sink of tropospheric hydroxyl radicals (OH). In clean tropospheric air (such as in remote marine and polar regions, as well as in most of the preindustrial atmosphere), most of the OH loss is by reaction with CO, and most of the rest by reaction with methane (CH_4) (e.g., Thompson, 1992). Changes in CO mole fraction ([CO]) can therefore impact numerous radiatively and chemically important atmospheric trace species, such as CH_4, non-methane hydrocarbons (NMHCs) and hydrochlorofluorocarbons (HCFCs) by influencing OH concentrations (e.g., Brasseur et al., 1999; Daniel and Solomon, 1998). Oxidation of CO by OH can also result in significant production of tropospheric ozone (e.g., Crutzen, 1973).

Given the important role CO plays in atmospheric chemistry, a good understanding of past changes in [CO] is required for a full understanding of the anthropogenically and naturally driven changes in global atmospheric chemistry as well as in trace gas budgets. The lack of reliable records of past [CO] has been a source of uncertainty for modeling studies of changes in atmospheric composition between the last glacial period, the preindustrial Holocene, and today (e.g., Crutzen and Brühl, 1993; Martinerie et al., 1995; Thompson et al., 1993). Model results of Martinerie et al. (1995), for example, suggested that in the preindustrial atmosphere, changes in [CO] were the most important factor influencing OH concentrations.

CO has both anthropogenic sources (combustion of fossil fuels, biofuels and biomass, oxidation of anthropogenic CH_4 and NMHCs) and natural ones (CH_4 and NMHC oxidation, wildfires), with the anthropogenic sources currently constituting more than half of the total (Table S5). Bottom-up inventories of anthropogenic CO emissions, e.g., RETRO, EDGAR-HYDE (Schultz and Rast, 2007; Schultz et al., 2008; van Aardenne et al., 2001), show significant disagreements, highlighting the uncertainties involved in such reconstructions. Such bottom-up CO emission inventories have been used in chemistry-transport models (CTMs) and typically underestimate [CO] in the northern extratropics (e.g., Shindell et al., 2006). These emission inventories are also being used in atmospheric chemistry models in support of climate model simulations for the IPCC 5th Assessment Report

(AR5) (Lamarque et al., 2010). Accurate [CO] reconstructions extending beyond the instrumental record can provide valuable constraints for these emission inventories and model simulations.

The average atmospheric lifetime of CO is only ≈ 2 months, and the source magnitudes and atmospheric mole fractions vary by latitude and differ greatly between the two hemispheres (Novelli et al., 1998b). For example, the recent ACCMIP emissions inventory estimates that the Northern Hemisphere (NH) anthropogenic CO emissions are $\approx 9 \times$ larger than Southern Hemisphere emissions (Lamarque et al., 2010). As a result of the large hemispheric imbalance in CO sources (both anthropogenic and, to a smaller degree, natural), the recent mean annual [CO] at Barrow, Alaska (71.32° N, 156.61° W), is $\approx 125\,\mathrm{nmol\,mol^{-1}}$, whereas for the South Pole it is $\approx 50\,\mathrm{nmol\,mol^{-1}}$. This means that the Northern Hemisphere and Southern Hemisphere (SH) [CO] histories need to be reconstructed separately. The NH is where the great majority of anthropogenic CO (and other anthropogenic trace gas) emissions occur and has therefore experienced the most dramatic changes in atmospheric composition and chemistry over the last several decades. The goal of this study is to reconstruct a reliable record of northern high latitude [CO] and thereby provide further constraints for CO emission inventories and atmospheric chemistry models.

The most comprehensive instrumental record of [CO] comes from the NOAA global flask network and extends back to 1988 (Novelli et al., 1998a; Novelli et al., 2003; Novelli et al., 1994). Flask measurements by the Oregon Graduate Institute (OGI) from a much smaller global network extend back to as early as 1979 for some sites (Khalil and Rasmussen, 1984; Khalil and Rasmussen, 1988; Khalil and Rasmussen, 1994). Figure 1 shows OGI and NOAA [CO] records from Barrow. Overlapping parts of these two records agree on the general decreasing [CO] trend in the early 1990s, although there are clearly some calibration scale offsets. The records suggest overall steady [CO] values in the 1980s, followed by a decrease in the early 1990s. Pre-1980 spectroscopic measurements of total atmospheric column CO at several locations are available and show a general trend of CO increase between about 1950 and 1980 (e.g., Rinsland and Levine, 1985; Yurganov et al., 1999). However, these measurements were more temporally and spatially limited and were made at sites that are closer to areas of high anthropogenic CO emissions than the NOAA and OGI measurements.

Extending the [CO] record beyond the period of instrumental measurements may be possible using old air preserved in glacial ice and firn. Firn is the uppermost layer of an ice sheet or a glacier and consists of compacted snow with an interconnected pore space. Gases move through the interconnected pore space slowly, primarily by molecular diffusion (e.g., Schwander et al., 1993). This results in an increase of the mean age of the gases and a broadening of the age
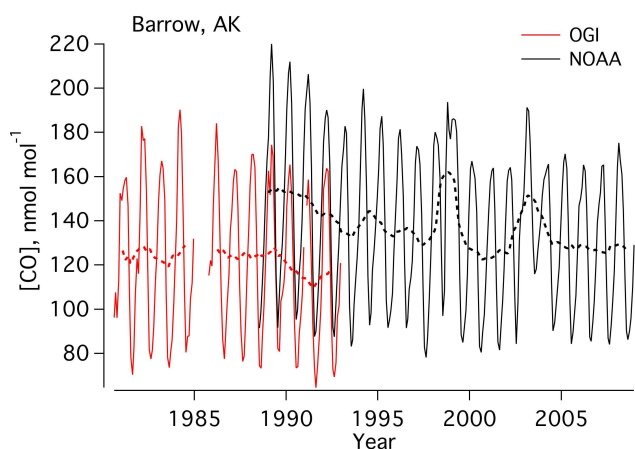
Fig. 1. Monthly mean records from flask measurements of [CO] by NOAA and OGI at Barrow, Alaska (solid lines). 12-month running means calculated from the monthly data are shown as dashed lines. OGI measurements are on the OGI scale, NOAA measurements are on the WMO-2004 scale. OGI data are from Khalil and Rasmussen (1984, 1988, 1994); NOAA data are from ftp://ftp.cmdl.noaa.gov/ccg.

distribution with depth in the firn (e.g., Rommelaere et al., 1997; Schwander et al., 1993; Trudinger et al., 1997). Toward the bottom of the firn layer, solid ice layers begin to form that almost completely impede vertical gas diffusion; this is known as the "lock-in zone" (e.g., Battle et al., 1996). Mean gas age increases rapidly with depth in the lock-in zone (e.g., Schwander et al., 1993; Trudinger et al., 1997). Air sampled from the firn can provide records back as far as 100 years at some sites such as the South Pole (e.g., Battle et al., 1996). Air trapped in the bubbles in fully closed ice below the firn layer can provide the atmospheric record farther back in time.

Prior to the firn CO work described here and in a companion paper (Wang et al., 2012), there was only one published study of Northern Hemisphere [CO] from firn air (Clark et al., 2007), and only two published studies from Greenland ice (Haan et al., 1996; Haan and Raynaud, 1998). The Clark et al. (2007) firn air record is from the small Devon ice cap in the Canadian Arctic and shows [CO] values generally increasing with depth in the firn, reaching a value of $186 \, \text{nmol mol}^{-1}$ for the oldest sample (mean year of origin = 1941). Such an increasing trend going back in time is unrealistic given growing anthropogenic emissions between 1940 and 1980, and suggests that CO is being produced in situ in the Devon firn. The Haan et al. (1996) and Haan and Raynaud (1998) studies were conducted on ice from the Greenland Summit area. These studies found [CO] decreasing gradually to $\approx 90 \, \text{nmol mol}^{-1}$ going back in time to ≈ 1850 AD, consistent with the expected trend of decreasing CO emissions going back in time (Lamarque et al., 2010). For air older than ≈ 1600 AD, however, they observed [CO] between 100 and $180 \, \text{nmol mol}^{-1}$, large variability and a

general increase going back in time, suggesting in situ CO production in deeper Summit ice. Several ice core and firn air studies of [CO] have also been done in Antarctica (Assonov et al., 2007; Ferretti et al., 2005; Haan et al., 1996; Haan and Raynaud, 1998; MacFarling Meure, 2004; Wang et al., 2010), although because of the relatively short atmospheric CO lifetime, these records do not provide much information about the [CO] trend in the NH high latitudes.

In this paper we present recent [CO] measurements from firn air at the NEEM ice core site in northern Greenland, as well as prior unpublished measurements from the Summit and NGRIP sites in central Greenland. Results from the NOAA global monitoring network indicate that mean annual [CO] is homogeneous within a few nmol mol^{-1} north of about 40° N (Novelli et al., 1998b); NOAA station [CO] data further indicate that [CO] over the Greenland ice sheet is representative of mean annual [CO] in the Arctic (Table S4). Our firn-based reconstruction is therefore expected to provide a [CO] history that is representative of clean background air for a large portion of the NH.

In the text below, sections accompanied by the Supplement are marked with an asterisk (*). Sections in the Supplement correspond to sections with the same number in the main text.

2 Sampling and analytical methods*

Firn air was sampled from three locations on the Greenland ice sheet (Fig. 2). All sampling locations were in clean, undisturbed snow and upwind (with respect to prevailing wind direction) from larger established camps and generators. The NEEM firn air campaign took place in July of 2008. Air was pumped primarily from two boreholes separated by 64 m and located at 77.43° N, 51.10° W. One of these was sampled to a depth of 77.75 m with a firn air system from the University of Bern (Schwander et al., 1993) and is referred to as "EU hole" in this manuscript. The second borehole was sampled to a depth of 75.6 m with a firn air system from the US (Battle et al., 1996) and is referred to as "US hole". More details on sampling procedure for EU and US boreholes can be found in Buizert et al. (2012).

A third borehole located ≈ 15 m from the US borehole was also sampled to a depth of 60 m near the end of the same campaign and is referred to as "S4". This borehole was sampled with a combination of the US firn air system (downhole assembly, purging pump/line and CO_2 monitoring) and a system from the Max Planck Institute for Chemistry in Mainz, Germany (high-capacity sampling pump and compressor) (Assonov et al., 2007).

Firn air was sampled from a single borehole (72.53° N, 38.28° W) near the Summit station in May–June 2006, using the US firn air system (Battle et al., 1996). Sampling at the NGRIP firn air site (75.1° N, 42.38° W) took place in
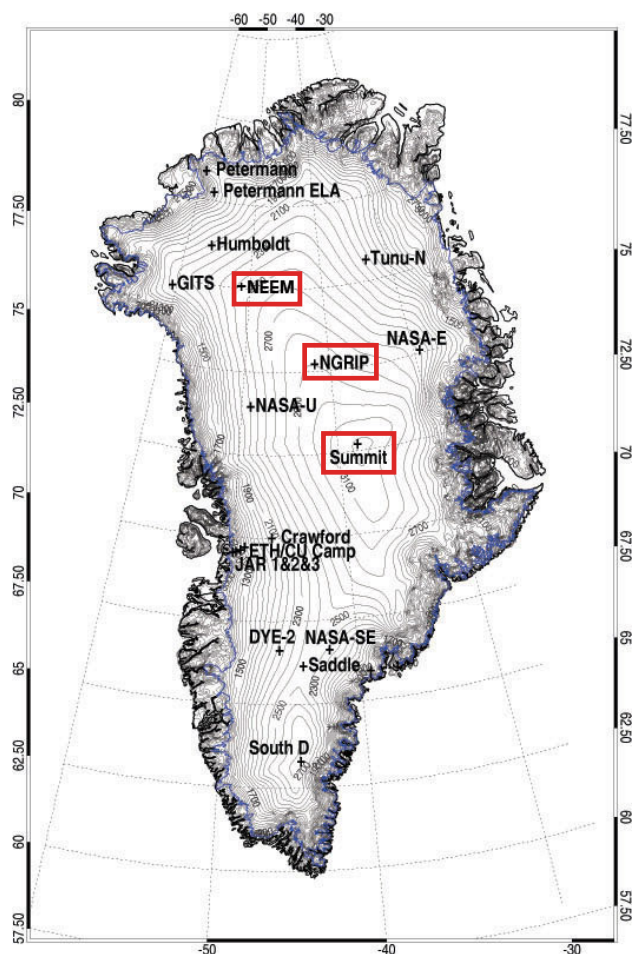
Fig. 2. Map of Greenland showing the locations of automated weather stations in the Greenland Climate Network (GC-Net), with the firn air sampling locations highlighted by red rectangles.

May–June 2001, using the University of Bern firn air system (Schwander et al., 1993).

Table S1 summarizes the firn air sampling as well as measurements relevant to this study. Five different institutions participated in the analyses, with all laboratories analyzing [CO] and four laboratories analyzing molecular hydrogen mole fractions ([H$_2$]). [H$_2$] is used below to help with the interpretation of the [CO] history.

For analyses at NOAA, air samples were collected into 2.5 L glass flasks from all boreholes and sites except NEEM S4. Samples from NGRIP and Summit were measured for [CO] using gas chromatography (GC) with hot mercuric oxide reduction detection (Novelli et al., 1992, 2003). Air collected at NEEM in 2008 was measured for [CO] using fluorescence in the vacuum ultraviolet (VURF, instruments from Aero-Laser GmbH, Garmisch-Partenkirchen, Germany). The CO mole fractions reported here are referenced to the WMO-2004 scale. The NOAA measurement uncertainty associated with each air sample was estimated from errors associated

with sample handling and analysis, differences between CO instruments, and the uncertainty in the scale internal consistency. The individual errors were propagated in quadrature. Firn samples measured in 2001 were assigned an uncertainty of 2.3 nmol mol^{-1} (equivalent to 1σ), 2.0 nmol mol^{-1} in 2006 and 1.2 nmol mol^{-1} in 2008. The reduced error in 2008 primarily reflects a change from GC analysis to VURF.

[H$_2$] in samples from NEEM was determined at NOAA using GC with a pulsed discharge helium ionization detector (Novelli et al., 2009). Overall [H$_2$] measurement uncertainties that include effects from sample handling and differences among instruments are ≈ 4 nmol mol^{-1}. The largest uncertainty in the measurements results from the [H$_2$] reference gases, which may drift over time (Novelli et al., 1999). The [H$_2$] measurements are referenced to the NOAA scale (Novelli et al., 1999).

Analyses of firn air at CSIRO were made on samples collected from the NEEM EU borehole in 0.5 L glass flasks. The air was pumped to a pressure of about 2 bar (absolute) after drying with magnesium perchlorate; the air collection technique is similar to the one used in CSIRO atmospheric sampling (Francey et al., 2003) and previous CSIRO firn air sampling (Etheridge et al., 1998). [CO] and [H$_2$] were analyzed using gas chromatography with a mercuric oxide reduction detector (Francey et al., 2003). The precision (1σ) of the [CO] and [H$_2$] measurements is ≈ 1.5 and 3 nmol mol^{-1} respectively. Uncertainties due to corrections for instrument response are within about 1 % over the range 20–300 nmol mol^{-1} for [CO] and 2 % over 430–1000 nmol mol^{-1} for [H$_2$]. CSIRO [CO] measurements are reported on an internal calibration scale that was originally linked to the NOAA scale via a high pressure cylinder standard at 196 nmol mol^{-1}. [H$_2$] measurements given here are on the CSIRO94 [H$_2$] scale. Intercomparison of CSIRO [CO] and [H$_2$] measurements with those made at NOAA (and other laboratories) is complicated by a number of observed systematic influences (Francey et al., 2003; Masarie et al., 2001), particularly for [CO] at lower mole fractions; [CO] scale offsets are thus not well characterized.

For analyses at Heidelberg University, samples were collected from the NEEM EU borehole into 6 L SilcoCan canisters (Restek Inc.), and from the NEEM US borehole into 2.5 L glass flasks. [CO] and [H$_2$] were analyzed using hot mercuric oxide reduction detection (RGA-3 instrument from Trace Analytical, Inc.); further details on the technique were described in Hammer and Levin (2009). The Heidelberg [CO] measurements are on the MPI Mainz scale, and the [H$_2$] measurements are on the MPI-BGC 2009 scale. The average 1σ analytical uncertainty for [CO] and [H$_2$] is typically ± 3 nmol mol^{-1}. The SilcoCan [H$_2$] analyses (EU borehole) yielded values that were obviously contaminated (likely due to outgassing from the SilcoCan canisters) and are not shown.

For analyses at Stony Brook, firn air samples were collected from the NEEM EU borehole in 3 L SilcoCan canisters

(Restek Inc.) at a pressure of 2.8 bar. [CO] and CO stable isotopic ratios (CO isotopic ratios are the subject of a companion paper (Wang et al., 2012)) were determined by cryogenic vacuum extraction, gas chromatographic separation, and continuous-flow isotope ratio mass spectrometry (CF-IRMS) using established methods (Wang and Mak, 2010). Further analytical details are found in Wang et al. (2012). The average 1σ analytical uncertainty for [CO] was 3.5 nmol mol^{-1}.

For analyses at University of East Anglia (UEA), firn air samples were collected from the NEEM S4 borehole into 8 L aluminum high-pressure cylinders; 1 sample from the NEEM US borehole was also collected. Analysis of [H$_2$] and [CO] was performed using a modified commercial reducing gas analyzer (RGA3, Trace Analytical, Inc., California, USA), described in detail in Forster et al. (2012). The inlet system was further modified to handle air from the compressed firn air samples as opposed to the routine atmospheric sampling described in Forster et al. (2012). Values are reported with reference to the MPI-2009 scale for [H$_2$] (Jordan and Steinberg, 2011) and WMO-2004 scale for [CO]. Measurement uncertainties (precision only, based on the standard deviation of three replicate analyses) are about 2 nmol mol^{-1} for [H$_2$] and 1 nmol mol^{-1} for [CO].

System blanks for [CO] and [H$_2$] were tested in the field for the EU and US firn air sampling systems used at NEEM. A cylinder of ultra-zero air, containing 4 nmol mol^{-1} of CO and 800 nmol mol^{-1} of H$_2$ was used to either directly fill glass flasks or to fill them via the firn air device by connecting the cylinder to the firn air device intake line. Flask flushing and filling procedure for these tests mimicked normal sample collection. These tests are shown in Table S2 and revealed no significant blank for [CO] for either sampling system. Small blanks of +4.8 nmol mol^{-1} (US system) and +6.1 nmol mol^{-1} (EU system) were found for H$_2$, significant at the 1σ but not the 2σ level.

An additional verification of the integrity of the sampling system for CO and H$_2$ comes from the comparison of surface ambient air samples taken with the firn air systems and ambient values observed at the nearest NOAA flask network sites. This comparison further indicates that the firn air systems do not have substantial blanks for CO and H$_2$ (see Fig. S1 and further discussion in the Supplement).

3 Firn air data

3.1 NEEM 2008 firn air data*

Figure 3 shows [CO] and [H$_2$] measurements from the NEEM 2008 firn air campaign as a function of depth below snow surface. [CH$_4$] from the US borehole is also included for reference, and shows the expected rapid decline with depth in the lock-in zone, indicating older air. [CO] depth profiles from all boreholes and all labs are in agreement on the main features, although there are clearly some calibration
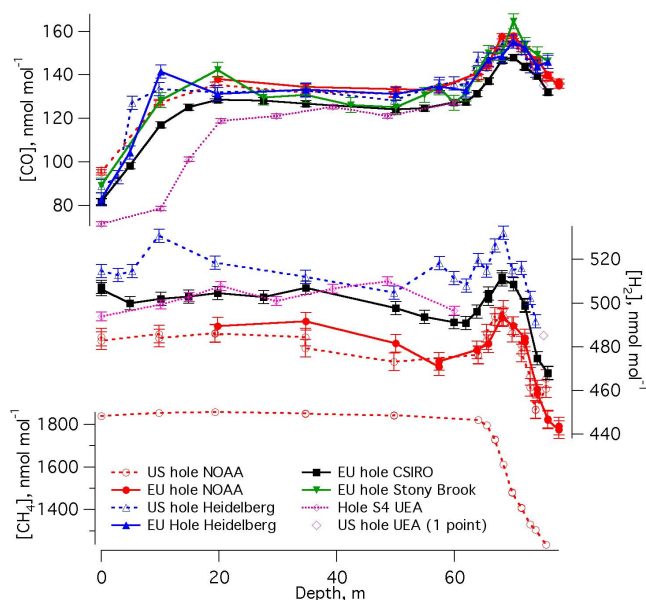
Fig. 3. Firn air measurements of [CO] and [H$_2$] from the NEEM 2008 campaign as reported by each laboratory. Error bars shown for NOAA and Heidelberg measurements represent overall 1σ uncertainty estimates; error bars for CSIRO, Stony Brook and UEA represent 1σ analytical precision only. [CH$_4$] is also shown for reference.

scale offsets. Low [CO] values observed at the surface and at the shallowest depths are explained by the Arctic summer [CO] minimum (e.g., Novelli et al., 1998b; Fig S3). Below the depth range of the seasonal signal (below ~ 40 m) and above the lock-in zone (lock-in starts at ~ 63 m, (Buizert et al., 2012)), [CO] stays nearly constant, as expected from the atmospheric [CO] trend in the Arctic for the several years preceding 2008 (Fig. 1). The oldest and most interesting part of the record is located below ≈ 63 m, in the lock-in zone. Here the measurements show a peak at ≈ 70 m depth, suggesting that the [CO] surface history at NEEM included an increase followed by a more recent decline. The S4 borehole was sampled about 2 weeks later than the EU and US boreholes, allowing the summer low [CO] values to propagate further into the firn. This process was likely enhanced by the relative proximity (≈ 15 m) of the open US borehole.

[H$_2$] depth profiles from all boreholes and all labs are also in agreement on the main features, although the calibration scale offsets for this gas appear to be larger. The [H$_2$] seasonal cycle is less pronounced than that for [CO] (e.g., Novelli et al., 1999). The depth profiles suggest a possible slight decrease in [H$_2$] toward the bottom of the diffusive zone, and, as for [CO], a peak (centered at ≈ 68 m) in the lock-in zone.

In order to reconstruct past atmospheric histories, we assembled the best-estimate combined data set for each borehole from the available data, taking two main (and somewhat conflicting) considerations into account. First, including data from more labs provides a more robust data set as well as

a more realistic measure of the full data uncertainty. Second, some data sets are clearly noisier than others, are difficult to place on the same calibration scale, or are otherwise more challenging for use in a historical reconstruction. Including these data sets can result in an unnecessary increase in uncertainties of the firn data as well as of the final atmospheric histories. With these considerations in mind, we excluded the Stony Brook and UEA [CO] data and the Heidelberg and UEA $[H_2]$ data from the combined data sets used for atmospheric reconstructions (see Supplement for details). Analyses and modeling of other species (Buizert et al., 2012) indicated that the gas age distributions are slightly different between the US and EU boreholes. For this reason we chose to treat these two boreholes separately for the atmospheric history reconstructions. The final combined NEEM data sets for [CO] and $[H_2]$ used for atmospheric history reconstructions are shown in Fig. 4 and Table S3. Further details on the final combined data sets can be found in the Supplement.
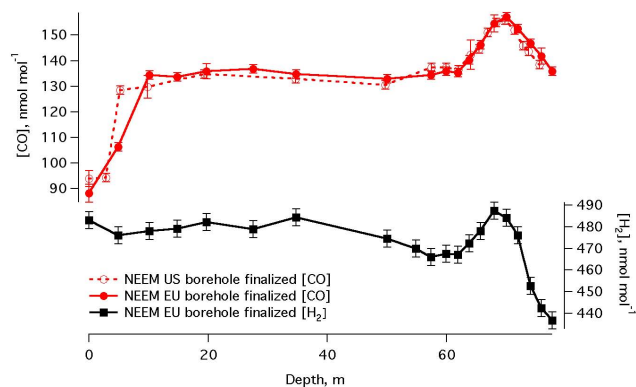
3.2 Summit 2006 and NGRIP 2001 firn air data

[CO] in flasks from the Summit 2006 and NGRIP 2001 campaigns was only measured at NOAA. Finalized data averaged for each depth level are shown in Fig. 5 and Table S3. The general features of these records are similar to NEEM. The observed surface [CO] depletion is smaller than at NEEM because of earlier sampling dates (late May to early June for both Summit and NGRIP, as compared to mid-July for NEEM). Because of the earlier sampling dates, the previous winter's [CO] maximum signal is shallower and more pronounced than at NEEM. Both Summit and NGRIP records show a similar [CO] peak in the lock-in zone. Note that the lock-in zone occurs deeper in Summit firn, causing the depth shift in the observed [CO] peaks. The difference in the depth at which the lock-in zone starts is illustrated by the $[CH_4]$ profiles. For the Summit site, the air at the deepest sampling level is younger than the deepest air from NEEM and NGRIP; this is evident from the higher $[CH_4]$ for the deepest Summit samples.

3.3 Is CO well preserved in Greenland firn air?*

We conducted a detailed examination of the data with regard to the possibility of in situ production of CO in Greenland firn. We first examined the possibility that the [CO] peaks observed in the lock-in zone at each site are due to in situ production from a widely deposited ice layer rich in trace organics. This hypothesis is easily rejected by considering ages of the ice layers that correspond to the depth of the CO peak at each site (see the Supplement).

Another way to examine whether an ice sheet gas record is well preserved is to compare records from several sites. Because [CO] is a relatively short-lived gas with heterogeneously distributed and temporally variable sources, small differences in its surface history between sites within Green-

Fig. 4. Finalized combined NEEM [CO] and $[H_2]$. [CO] is on WMO-2004 scale, $[H_2]$ is on the NOAA scale.
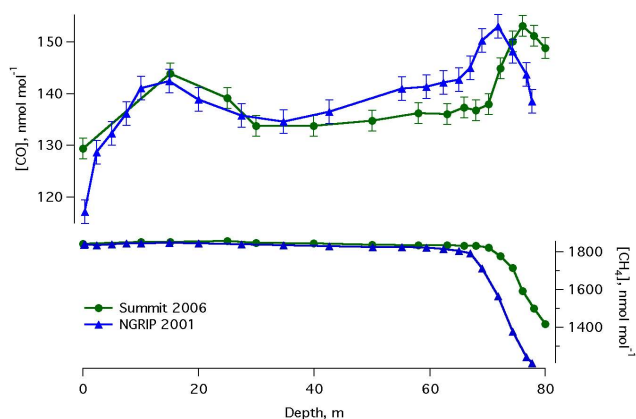
Fig. 5. Finalized [CO] data from the Summit 2006 and NGRIP 2001 firn campaigns. $[CH_4]$ measured at NOAA is also shown for perspective. All [CO] data are on the WMO-2004 scale. The error bars represent NOAA overall measurement uncertainties.

land may be possible. The NOAA flask sampling sites most likely to be representative of [CO] over Greenland are Summit (within 5 km of Summit firn air site), Alert in the Canadian Arctic (82.45° N, 62.51° W), Barrow in northern Alaska (71.32° N, 156.61° W) and Ny-Ålesund in Svalbard (78.90° N, 11.88° W). There are indeed some small differences (up to 2 nmol mol^{-1} overall) in mean annual [CO] between these sites, with overall highest values at Ny-Ålesund and lowest values at Summit (Table S4). The Summit site also appears to have a reduced seasonal cycle (by as much as 20 nmol mol^{-1} in amplitude) as compared to the other sites.

Despite these differences, we would expect the time-smoothed [CO] histories (which is what the firn air contains) to be generally consistent between our firn sites. In order to make this comparison, the firn air measurements from the three sites need to be placed on a common timescale. Prior to conducting full model-based atmospheric history reconstructions, this is possible by plotting [CO] against $[CH_4]$. CH_4 is well preserved in ice and firn at inland Greenland sites,

and the free-air diffusivities of CO and CH_4 are fairly similar (9 % smaller for CO than for CH_4 at the $-28.9\,°C$ mean-annual temperature for NEEM) (Buizert et al., 2012). This results in very similar age distributions with depth for CO and CH_4, as illustrated in Fig. S2. If in situ CO production is indeed a significant problem, we would expect to see some differences, as these sites do have slightly different mean annual temperatures and likely different distributions of organics with depth (because of differences in snow accumulation rates and likely differences in deposition rates of organics).

Figure 6 presents the [CO]–[CH_4] plots for all boreholes. To ensure the comparison is as meaningful as possible, only data from the lock-in zone of each borehole are plotted. Above the lock-in zone, the age distributions are narrower and younger (e.g., Schwander et al., 1993). Because NEEM was sampled 2 yr later than Summit and 7 yr later than NGRIP, some NEEM depth levels above the lock-in zone contain CO age distributions that are not matched at all at Summit and especially at NGRIP. Figure 6 shows generally good agreement between the three sites, consistent with the hypothesis that CO is well preserved in the firn at inland Greenland sites. Peak [CO] values appear to be higher by $\sim 5\,nmol\,mol^{-1}$ in NEEM EU than in Summit and NGRIP, which may be explained by a number of factors as discussed below and in the Supplement.

We also examined the question of whether the firn air [CO] values are well predicted by the known [CO] surface histories from direct atmospheric measurements. [CO] data for about the last two decades are available for several Arctic sites from the NOAA global flask network (Novelli et al., 1998). Further, OGI [CO] data for Barrow are available back to 1980 (Fig. 1). We can run the firn gas transport models (see Sect. 4.1) using the direct atmospheric measurement time series as input and compare the firn model output with observed values for all boreholes (Fig. 7). Such a comparison is only valid to a limited depth in the firn, however. In Fig. 7, we stop the model curves at the depths at which the CO mean year of origin (commonly referred to as "mean age") equals the year in which the atmospheric measurements began at a given site.

Figure 7 shows model-produced curves from NOAA Alert and Ny-Ålesund station histories, as well as from a combined NOAA–OGI Barrow history (see Supplement). The NOAA Summit station record is not used because it is shorter and contains large gaps. As can be seen, model curves match NGRIP and Summit firn air data well within uncertainties, but there are offsets of up to $5\,nmol\,mol^{-1}$ for NEEM, with firn data higher than the model curves. The offsets do not, however, show an increasing trend with depth as would be expected for gradual in situ CO production. It is possible that the meteorology at the firn air sites results in a slight weighting of the firn air signals toward the winter, when surface [CO] is much higher, and that this winter bias is greatest at NEEM (Supplement text, Fig. S3). Our conclusion is that the firn air [CO] signals are overall representative of the Green-
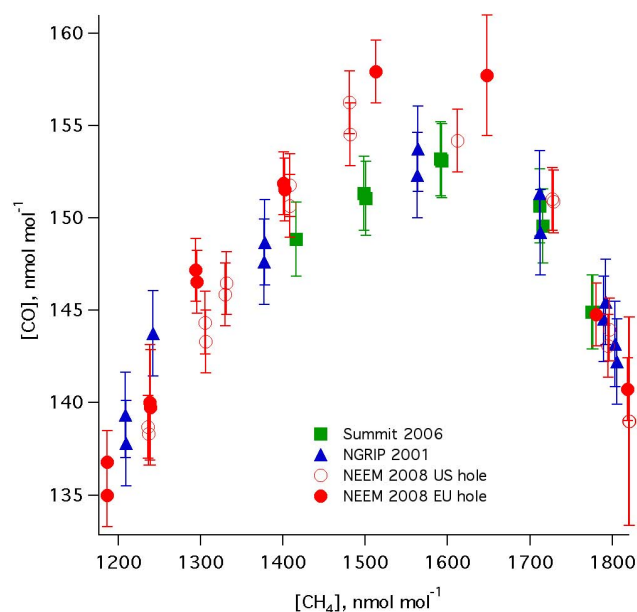
Fig. 6. A plot of finalized [CO] vs. [CH_4] from each firn air borehole considered in the study. All [CO] data are on the WMO-2004 scale.

land surface [CO] history, although we cannot completely rule out a small contribution from in situ CO production (up to $5\,nmol\,mol^{-1}$).

4   Firn gas transport modeling and [CO] history reconstructions

4.1   Forward modeling*

Depth–mole fraction profiles in firn air contain atmospheric trace gas histories that have been smoothed by gas movement in the firn (e.g., Schwander et al., 1993). The gas movement needs to be characterized and depth–age distributions determined before atmospheric reconstructions are possible. This first step is accomplished via the use of "forward" gas transport models. Such models take a surface gas history as input and produce a depth–mole fraction profile for a specified sampling date (e.g., Battle et al., 1996; Rommelaere et al., 1997; Schwander et al., 1993; Trudinger et al., 1997).

Two forward gas transport models were used in this study: the LGGE-GIPSA model (Witrant et al., 2012) and the IN-STAAR model (Buizert et al., 2012). Both models allow for diffusive and advective gas transport in the firn, and both performed very well in a recent intercomparison of six firn air models for the NEEM site (Buizert et al., 2012).

Both the INSTAAR and the LGGE-GIPSA models were used for characterizing firn air CO for the NEEM EU and US boreholes. The free-air molecular diffusivities used for each gas species are as in Buizert et al. (2012). The effective diffusivities for each depth level were tuned to a suite of long-lived gases with well-constrained atmospheric histories.
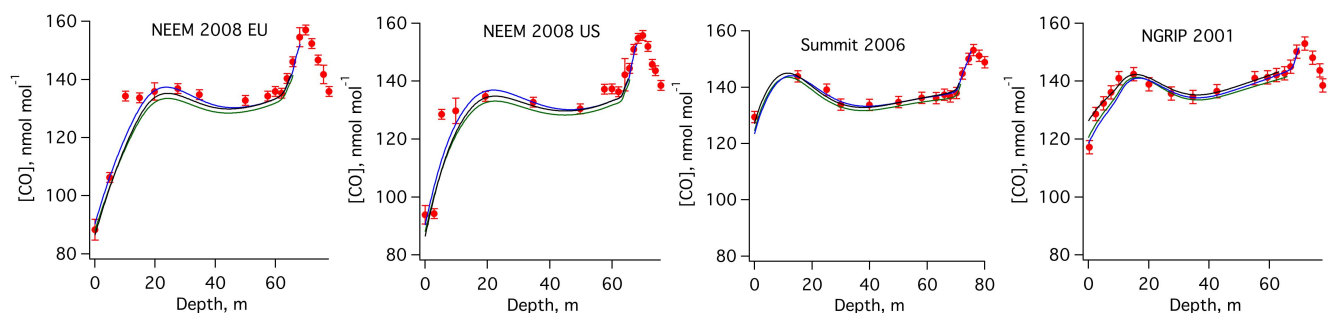
Fig. 7. Comparison of firn [CO] data with firn forward model runs (LGGE-GIPSA model) using atmospheric measurements from Arctic stations. Data are in red (WMO-2004 scale, with uncertainties). Color scheme for model runs: NOAA + OGI Barrow history – blue; NOAA Alert history – green; and NOAA Ny-Ålesund history – black.

This tuning procedure involves iteratively running all the gas histories through the model and minimizing the overall data–model mismatch for all the firn data points. CO_2, CH_4, SF_6, CFC-11, CFC-12, CFC-113, HFC-134a, CH_3CCl_3 and $\delta^{15}N_2$ were used as the tuning gases for NEEM EU, and CO_2, CH_4, SF_6 and $\delta^{15}N_2$ were for NEEM US (Buizert et al., 2012). Because both models are able to simultaneously reproduce the firn depth profiles of gases with a range of histories, from monotonic increase (e.g., CO_2) to peak and rapid decline (e.g., CH_3CCl_3), we have high confidence in the ability of these models to accurately characterize firn air CO.

Only the LGGE-GIPSA model was used for characterizing firn air CO for the Summit and NGRIP sites. CH_4, SF_6, CH_3CCl_3, CFC-11, CFC-12, CFC-113 and HFC-134a were used for diffusivity tuning for Summit, and CO_2, CH_4, SF_6, CH_3CCl_3, CFC-11, CFC-12 and CFC-113 were used for NGRIP. A more detailed presentation of firn air characterization at these two sites is found in Witrant et al. (2012).

CO age distributions at different depth levels (Fig. S2) are predicted by forward models by running an atmospheric history that is zero at all times except for a 1-month-long square wave of magnitude 1 at the beginning.

4.2 Inverse modeling and [CO] scenario generation*

The depth–age distribution matrices generated by the forward models and the measured depth–[CO] profiles together contain the information needed to reconstruct the surface [CO] history. Following Rommelaere et al. (1997), we refer to the depth–age distribution matrices as "transfer functions". Convolving an atmospheric time trend with such transfer functions is equivalent to using the atmospheric time trend as input to the forward firn models (Rommelaere et al., 1997). The theoretical approach for time trend reconstruction used in this study (Rommelaere et al., 1997) effectively performs the inverse of this convolution. The inverse scenarios are limited in their resolution of fast changes and cannot correctly reconstruct the large [CO] seasonal cycle. This presents a technical difficulty for the inverse model because [CO] in the upper ∼ 40 m in the NEEM firn is significantly influenced

by the large seasonal variations at the surface (Wang et al., 2012). We therefore corrected the [CO] data in the upper firn to remove seasonal effects prior to applying the inverse model (Wang et al., 2012). This adjustment has no significant effect on [CO] in the deeper firn, which contains all the information on the pre-1990 [CO] history (our main interest).

The firn gas inverse problem is underconstrained, and a regularization term controlling the smoothness of the scenario must be prescribed to obtain a unique solution (e.g., Aydin et al., 2011; Rommelaere et al., 1997). Scenarios that have low smoothing produce the best match to the data, but such scenarios include an unrealistic amount of short-term variability (more information than is contained in the firn). Scenarios that have too much smoothing do not match the firn data well. Rommelaere et al. (1997) adjusted the regularization term using a chi-square test based on the a priori experimental error. An important limitation of this method is that the a priori uncertainty is difficult to assess precisely, especially for multisite simulations which are sensitive to differences between single site data series (e.g., intercalibration biases or geographic variations). Thus we defined an optimal solution by using model estimates of uncertainties; the stability of such solutions is then explored by varying the weight of the regularization term around its optimal value (Wang et al., 2012; Sapart et al., 2013). More precisely, an optimal solution is defined as the minimum of the sum of two error terms: (1) the uncertainty based on the covariance matrix of the reconstructed scenario (Eq. 36 and Fig. 12 in Rommelaere et al., 1997), which decreases when the regularization term increases, and (2) the mean squared deviation between model results and data, which increases when the regularization term increases. Tests performed on multiple species showed that using this minimum as the optimal solution provides more stable results (in terms of realistic scenario smoothness) than trying to exactly match the experimental error estimate, which is uncertain (as was done in Rommelaere et al., 1997). More recently, a new robustness-oriented definition of the optimal solution has been implemented in our model (Witrant and Martinerie, 2013); it provides results consistent

with the range of CO scenarios obtained originally (Fig. S4). The inverse model can also be used in multisite mode, in order to infer an atmospheric scenario that fits several firn data sets (Rommelaere et al., 1997; Sapart et al., 2013).

A two-step approach was adopted in this study in order to explore the interplay between non-modeled uncertainties and mathematical underdetermination of the problem: reasonably smooth scenarios are tested through all available data sets and models. This allows us to indirectly take into account model uncertainties based on the use of both the IN-STAAR and LGGE-GIPSA models and possible geographic variations of [CO] between the three modeled Greenland sites. First, families of scenarios (with different regularization terms) were generated using data and the transfer functions from both models for all individual sites, as well as using multisite reconstructions. All scenarios were then tested by convolution with all available transfer functions; for the NEEM boreholes the scenarios were tested with transfer functions from both the INSTAAR and LGGE-GIPSA forward models, for Summit and NGRIP with transfer functions from the LGGE-GIPSA model only.

We required that all the data points below 40 m depth at all sites were matched within the combined data–model uncertainties. The combined data–model uncertainty was defined as

$$\sqrt{(2\sigma)^2 + (1.4\ \mathrm{nmol\ mol}^{-1})^2} + 1\ \mathrm{nmol\ mol}^{-1},$$

where σ is the estimated 1-sigma data uncertainty; $1.4\ \mathrm{nmol\ mol}^{-1}$ is the estimated uncertainty arising from the forward models themselves, and $1\ \mathrm{nmol\ mol}^{-1}$ is the estimated additional uncertainty arising from possible average atmospheric history differences between the sites (due to geographic variations in atmospheric [CO]). We used 2σ (rather than 1σ) data uncertainties because we required that all the data points are matched in these tests (statistically, the 1σ envelope only includes $\sim 68\%$ of Gaussian data). We added the possible $1\ \mathrm{nmol\ mol}^{-1}$ geographic offset linearly rather than quadratically because it represents a systematic bias rather than random error.

We allowed a single exception to the "all data points below 40 m must be matched" rule for the NGRIP data point at 42.6 m depth. The deseasonalized atmospheric trend at Barrow shows an important anomaly in 1998–1999 (see Fig. 1), which is likely due to a large biomass burning event (e.g., van der Werf et al., 2006). Forward model tests showed a strong impact of this anomaly on concentrations in firn down to the lock-in depth at NGRIP, which was sampled in 2001. Thus the inability of the model to produce scenarios that match the NGRIP data point at 42.6 m depth is likely due to this brief anomaly. Without this exception, a large number of reconstructed CO scenarios would be excluded (Fig. S4). Excluding these scenarios would not significantly affect our overall scenario envelope, as other very similar scenarios are not excluded (Fig. S4). However, most of the two-site scenarios

based on NEEM EU + NEEM US data would be excluded. As overall the firn at NEEM is probably the best characterized of all sites (more species, replicate measurements from more labs and overall more recent, higher-quality analyses), we decided to make the exception for this data point to retain the NEEM-based scenarios.

A combined root-mean-square deviation (RMSD) value was calculated for each scenario after convolutions with all the transfer functions for all sites. To produce a reasonable number of final scenarios, we accepted scenarios that were not more than 15 % higher in their RMSD than the best RMSD scenario. Some scenarios generated with low values of the regularization term (visibly too irregular) were still able to pass the data–model comparison test, indicating that even a multisite approach with two models still left the inverse problem underdetermined. We excluded the scenarios having a lower than optimal regularization term as they show higher-frequency temporal information than what is actually contained in the firn. A recent revision of the optimal solution that takes into account the sparsity of measurements in the definition of the regularization term based on stochastic analysis (Witrant and Martinerie, 2013) confirmed the validity of this intuitive criterion (see Supplement). Convolutions of the final successful set of 61 scenarios with the transfer functions for each site and each model are shown in Fig. S5.

The reliability of the scenarios decreases gradually going back in time, as fewer CO molecules from a given year remain in the sampled open porosity of the firn. There is thus a need to identify the earliest date at which the scenarios are considered "meaningful". One approach that has been used for this in the past is defining the earliest date for which the scenarios have at least 50 % reliability as the mean age at the depth where the open/total porosity ratio is 50 % (Sowers et al., 2005; Bernard et al., 2006). Another approach is to simply use the mean age at the deepest sampled level as the earliest meaningful scenario date. Both of these approaches give similar results, allowing us to reconstruct Greenland surface [CO] to ≈ 1950.

Inverse modeling techniques may allow us to take into account prior information such as the available CO atmospheric data since 1980 (e.g., Trudinger et al., 2002). As this option is not yet available in our inverse model, we alternatively tested the consistency of atmospheric and firn data using the forward firn model (Fig. 7). This strategy has the benefit of allowing an evaluation of the model from measurements that are not involved in the inverse problem solution, which is essential for model checking (e.g., Ljung, 1999). The good consistency obtained suggests that our inverse scenarios overall would not change significantly if the direct atmospheric measurement constraint was added to the firn data constraint.

5 Reconstructed [CO] history and discussion

5.1 Reconstructed [CO] history over Greenland

Figure 8 shows the final set of 61 scenarios for Greenland surface [CO] history. The most prominent feature of both the firn-depth profile and the reconstructed history is the well-characterized peak in [CO] over Greenland that occurs before the start of the NOAA [CO] monitoring. Our reconstruction suggests mean annual values of ≈ 140–$150\,\mathrm{nmol\,mol^{-1}}$ in 1950, already higher than those in the last decade ($\approx 130\,\mathrm{nmol\,mol^{-1}}$). [CO] increased by 10–$15\,\mathrm{nmol\,mol^{-1}}$ from 1950 to a peak in the late 1970s. After ≈ 1980, [CO] declined by $\approx 30\,\mathrm{nmol\,mol^{-1}}$ to values observed in the last few years.

As discussed above, reconstructing gas histories from firn is an underconstrained problem, and a significant range of [CO] peak dates is possible. The uncertainty in the [CO] peak date is captured by the peak date variability between the different scenarios. The [CO] peak date shows a dependence on scenario smoothness, with the smoothest scenarios giving the earliest peak dates. The peak date is also dependent on the boreholes used for the reconstruction. Scenarios based on the NEEM boreholes (pink, orange, red lines in Fig. 8) give the earliest peak dates, while multisite (NEEM + Summit + NGRIP) scenarios (light and dark green lines) give the latest peak dates. Scenarios reconstructed using transfer functions from the INSTAAR model (dashed lines) give peak dates that are earlier by a few years compared to scenarios using LGGE-GIPSA transfer functions (solid lines) for the same boreholes. The peak date dependence on the model and site combination still remains when the new definition of the optimal solution from Witrant and Martinerie (2013) is used (Fig. S4). Thus, uncertainties in model representation of firn physics likely dominate the uncertainty in the optimal inverse solution for the [CO] peak date. This variation in the [CO] peak dates highlights the importance of using multiple sites and models to fully capture the uncertainties in firn air reconstructions.

Overall, based on the full set of 61 scenarios, we constrain the [CO] peak date to between 1971 and 1983. The average scenario has the [CO] peak in 1976. As our reconstructed [CO] history is highly smoothed, it is not necessarily in conflict with the OGI Barrow data, which indicate steady [CO] in the 1980s followed by a decline in the 1990s. It is possible, for example, that the true atmospheric trend had highest [CO] in the early 1970s, an overall decline to 1980, and a [CO] plateau during the 1980s.

The reconstructed [CO] history can reflect changes in CO source magnitude, source distribution, transport, sink strength, or any combination of these. To thoroughly explore the implications of the reconstructed history for this short-lived gas, a state-of-the-art atmospheric chemistry model (including climatology) capable of repeated long historical runs is needed. Such a model is not available to us at this time, al-
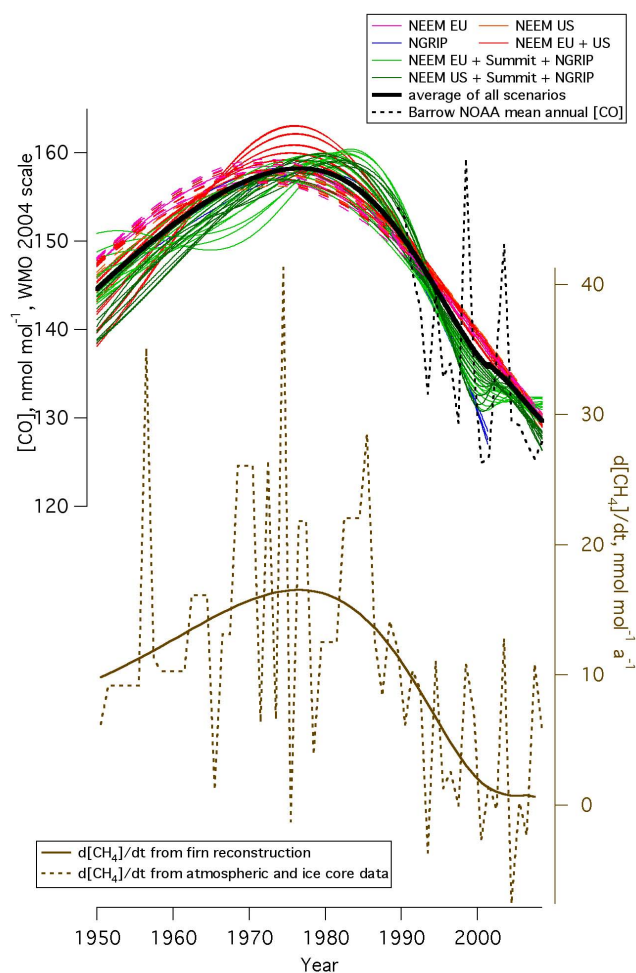
Fig. 8. Upper part: the final set of reconstructed scenarios (61 total) for Greenland surface [CO]. Different colors identify the firn air boreholes (single or multiple) that were used to reconstruct each scenario. Solid lines are used to plot scenarios derived from transfer functions obtained with the LGGE-GIPSA model; dashed lines denote scenarios derived from transfer functions obtained with the INSTAAR model. Average of all scenarios is plotted as a thick black line. For comparison, the NOAA Barrow [CO] history (mean annual) from flask measurements is shown as a black dashed line. Lower part: $\mathrm{d[CH_4]/d}t$ history estimated for NEEM. The solid $\mathrm{d[CH_4]/d}t$ line is based on a multisite reconstruction (NEEM-EU, NGRIP, Summit) of $[CH_4]$ using the LGGE inverse model. The dashed line (1 yr $\mathrm{d[CH_4]/d}t$ estimates) is based on a previously described (Buizert et al., 2012) $[CH_4]$ history compiled for NEEM from NOAA flask data and high-resolution data from the Law Dome firn air and ice core site (Etheridge et al., 1998).

though we do present a comparison with one historical model run that was recently completed (Lamarque et al., 2010). We therefore limit ourselves to a mostly qualitative discussion of the [CO] history, comparing it with histories of other trace gases and isotopic constraints related to CO sources or sinks. Our main focus is the [CO] history before 1990, as after 1990

global [CO] is very well characterized by the NOAA monitoring network.

5.2 Comparison with the methane change rate

To investigate the possible role of OH in the derived [CO] history, we compared the [CO] history with the rate of [CH$_4$] change over the same time interval. Both atmospheric CO and CH$_4$ are removed primarily by OH, although CH$_4$ has a much longer lifetime of ≈ 9 yr. While changes in OH concentration would result in a [CH$_4$] response that is delayed compared to a [CO] response, d[CH$_4$]/dt would be expected to respond relatively quickly. One complication involved with the [CO]–d[CH$_4$]/dt comparison is that CH$_4$ removal by OH is also a large source of CO (currently $\approx 1/3$ of the global CO source, (Duncan et al., 2007). Increasing OH would therefore increase not just the CO sink but the source as well; the sink effect however is more important.

Figure 8 shows a comparison of [CO] histories with d[CH$_4$]/dt estimated at NEEM. For this comparison, we estimated the d[CH$_4$]/dt history in two different ways. First, the solid d[CH$_4$]/dt line in Fig. 8 is determined from a multisite (NGRIP, Summit, NEEM-EU) firn inversion of [CH$_4$] using the LGGE inverse model. This model-based reconstruction provides a d[CH$_4$]/dt history that is smoothed by the same firn gas transport processes as the [CO] history. Second, the dashed line in Fig. 8 represents d[CH$_4$]/dt that is based on a [CH$_4$] atmospheric history for NEEM as estimated from NOAA flask data as well as Law Dome high-resolution ice core and firn air data (Etheridge et al., 1998); a more detailed discussion of this [CH$_4$] atmospheric history estimate is presented in Buizert et al. (2012). Based on the uncertainties in the NOAA and Law Dome-based [CH$_4$] history, we estimate the uncertainty in the d[CH$_4$]/dt peak date to be about ± 10 yr.

Figure 8 suggests that [CO] and d[CH$_4$]/dt peak dates for the high northern latitudes coincide; however, given peak date uncertainties for both species, offsets are possible. Studies of global [CH$_4$] trends during the observational period have usually attributed the d[CH$_4$]/dt decline during the 1980s to stabilizing anthropogenic emissions (e.g., Dlugokencky et al., 2003). One explanation for the similarity between the [CO] and d[CH$_4$]/dt trends during the entire 1950 to 2010 period is then simply that changes in CO and CH$_4$ sources are responsible. CO and CH$_4$ are co-emitted to a significant extent only from biomass burning (e.g., Duncan et al., 2007; Mikaloff-Fletcher et al., 2004), but wildfire emissions likely increased, rather than decreased during late 1970s and 1980s (Schultz et al., 2008). The long-term similarity in the [CO] and d[CH$_4$]/dt trends would therefore have to be explained by coincident changes in largely independent (likely anthropogenic) sources of each gas.

The [CO] and d[CH$_4$]/dt trends are also qualitatively consistent with an alternative hypothesis that involves a significant role of long-term changes in OH. While OH changes seem unlikely to explain the observed trends after about 1985, OH changes prior to about 1985 are less well constrained (see Sect. 5.4). A quantitative exploration of this hypothesis would require repeated historical CTM runs and is beyond the scope of this work. Figure 8, however, highlights that changes in OH may need to be considered for understanding the [CO] and d[CH$_4$]/dt trends for the earlier part of the record.

5.3 Comparison with records of light hydrocarbons from Greenland firn air

A record of ethane from Summit firn air (Aydin et al., 2011) as well as records of multiple light hydrocarbons from NGRIP (Worton et al., 2012) and NEEM (Helmig et al., 2013) have recently been published. All of these records consistently show large lock-in zone peaks for all species at all sites, and they are consistently reconstructed (by three different firn gas models) to produce histories with atmospheric peaks around or a few years before 1980, similar to [CO]. One exception is the NEEM ethane record, which places the atmospheric peak closer to 1970 (Helmig et al., 2013).

These light hydrocarbons share some important sources with CO, such as fossil fuel combustion (e.g., Pozzer et al., 2010), biofuel combustion (e.g., Xiao et al., 2008) and biomass burning (e.g., Simpson et al., 2011). The major sink for these hydrocarbons is OH (e.g., Helmig et al., 2009), similar to CO. As for CH$_4$, the oxidation of these light hydrocarbons in the atmosphere leads to CO production (see Table S5).

The hydrocarbon reconstructions show large decreases in mole fractions over Greenland in the two decades following the peak values around 1980. For example, butanes and pentanes decline by around 50 % from 1980 to 2000 (Worton et al., 2012), while ethane declines by 25–35 % (Aydin et al., 2011; Worton et al., 2012). Worton et al. (2012) attribute the hydrocarbon decline at least partly to reductions in emissions from road transportation associated with the introduction of catalytic converters, starting in the 1970s. Because catalytic converters also remove CO, this explanation is qualitatively consistent with the observed [CO] trend. A decline in atmospheric hydrocarbons would also result in a decrease in the oxidation source of CO, again consistent with the observed coincidence of [CO] and hydrocarbon atmospheric peaks over Greenland.

5.4 OH variability before 1990 inferred by other studies

Several studies exist on variability in OH concentrations that extend back to years before 1990. Most of these studies use data from the ALE/GAGE/AGAGE atmospheric monitoring of methyl chloroform (CH$_3$CCl$_3$), which began in 1978 (Prinn et al., 1992; Prinn et al., 1995; Prinn et al., 2005). Because CH$_3$CCl$_3$ is removed almost entirely by OH, its

atmospheric mole fractions can be used to deduce OH if the emissions are well constrained.

Prinn et al. (2001) estimated a large (up to 30 %) increase in NH OH between 1979 and 1990, and a ∼ 15 % increase in globally averaged OH during the same time, although the reason for this increase was unclear. The errors on these OH estimates are relatively large and allow for a situation with essentially no trend even for the NH. Krol and Lelieveld (2003) used the same CH_3CCl_3 atmospheric data to independently estimate similar OH increases (both for the NH and globally) from 1979 to 1990. Bousquet et al. (2005) also used the ALE/GAGE/AGAGE CH_3CCl_3 data and inferred global OH variations that were similar to those from the Krol and Lelieveld (2003) and Prinn et al. (2001) studies. Both the Krol and Lelieveld (2003) and the Bousquet et al. (2005) studies emphasized, however, that the OH inversions are very sensitive to errors in CH_3CCl_3 emission estimates used in the models.

Dentener et al. (2003) used a different approach and employed a CTM to estimate a very small positive global OH trend of 0.24 % a^{-1} for the 1979–1993 period based on modeling the CH_4 source/sink balance.

A recent study by Montzka et al. (2011) provided strong evidence for very small (5 % or less) global OH variability inferred from observations of multiple trace gases as well as from atmospheric chemistry model simulations. This study argued that earlier estimates of large OH variability from CH_3CCl_3 observations for years before 1998 (studies mentioned above) were affected by the relatively large uncertainties in CH_3CCl_3 emissions for those years. While the Montzka et al. (2011) study focused primarily on OH variability after 1998, it did also provide an estimate based on CH_4 observations back to 1985. This estimate showed similarly small OH variability of only a few percent during the entire 1985–2008 period considered. Overall, the Montzka et al. (2011) study provided convincing evidence that global average OH is well buffered, with large changes being unlikely.

We note that there are some limitations on the insights that can be gained from comparing independent OH reconstructions with our reconstructed Greenland [CO]. The OH reconstructions are global or hemispheric averages, with OH being most abundant in the tropics (e.g., Spivakovsky et al., 2000), whereas the latitude band that is of most importance for Greenland CO is considerably narrower, likely ≈ 30–90° N, because of the relatively short CO atmospheric lifetime.

5.5 Comparison with [H_2] in NEEM firn air*

A further intriguing but highly speculative piece of supporting evidence comes from the [H_2] measurements in NEEM firn air (Figs. 3 and 4). As we are not aware of any prior published firn air [H_2] measurements, we describe these here in some detail. CO and H_2 have similar sources and are usually co-emitted (or co-produced, in the case of hydrocarbon oxidation), although the CO : H_2 emission or production ratio is variable (Duncan et al., 2007; Price et al., 2007; Table S5). The sinks of CO and H_2, on the other hand, are very different. While OH is the dominant sink for CO, H_2 is primarily removed by soil uptake. Synchronous changes in [CO] and [H_2] would thus be more consistent with changes in the sources, while decoupled changes would be more consistent with changes in the sink. An increase in the OH concentration would be expected to lead to an almost immediate corresponding decline in [CO]. The resulting decline in [H_2], on the other hand, would be expected to be much smaller due to the much lower fraction of H_2 that is removed by OH. The [H_2] decline would also be expected to be delayed with respect to [CO]. This is due to the longer lifetime of H_2, as well as to the fact that initially the CH_4 oxidation source of H_2 will increase in response to an OH increase, and may entirely cancel or even temporarily overwhelm the effect of the increased OH sink.

Compared to CO, H_2 presents an additional difficulty with respect to firn air reconstructions. The molecular diameter of H_2 is small enough that it is expected to diffuse through the ice lattice at non-negligible rates (e.g., Severinghaus and Battle, 2006). The exact rates of H_2 diffusion in ice are unknown and effects on firn air concentrations have not been quantified. One expected effect is a slight increase in the effective firn diffusivities of H_2, resulting in actual age distributions being younger than those predicted by our models, particularly in the lock-in zone. An alternative way to conceptualize this is that the increased effective diffusivity of H_2 would result in a transient atmospheric [H_2] peak being recorded (as a peak) deeper in the lock-in zone.

Another important effect is an expected progressive enrichment of [H_2] with depth in the lock-in zone due to bubble close-off fractionation (Severinghaus and Battle, 2006). For example, $a > 90$ ‰ (≈ 9 %) enrichment in the Ne / N_2 ratio was observed at the bottom of the lock-in zone at the South Pole, and Ne and H_2 have a very similar molecular diameter (Severinghaus and Battle, 2006). Because of the expected enrichment with depth, bubble close-off fractionation would have the effect of raising [H_2] and shifting the observed [H_2] peak deeper in the lock-in zone.

These expected but unquantified H_2 effects in the firn preclude a reliable history reconstruction at this time. However, both of the described effects are expected to shift the observed [H_2] peak deeper in the lock-in zone. In our model history reconstruction, the atmospheric [H_2] peak would thus appear older than in reality. So while we cannot reconstruct a reliable history, we may be able to constrain the oldest possible date of the atmospheric [H_2] peak. Figure 9 shows a comparison of [H_2] and [CO] reconstructions from the NEEM EU borehole. As can be seen, [H_2] peaks significantly (at least a decade) after [CO], even though we expect the [H_2] peak to be old-shifted. This delay in the [H_2] peak with respect to [CO] is consistent with OGI atmospheric monitoring (Khalil and Rasmussen, 1990), which shows [H_2] continuing
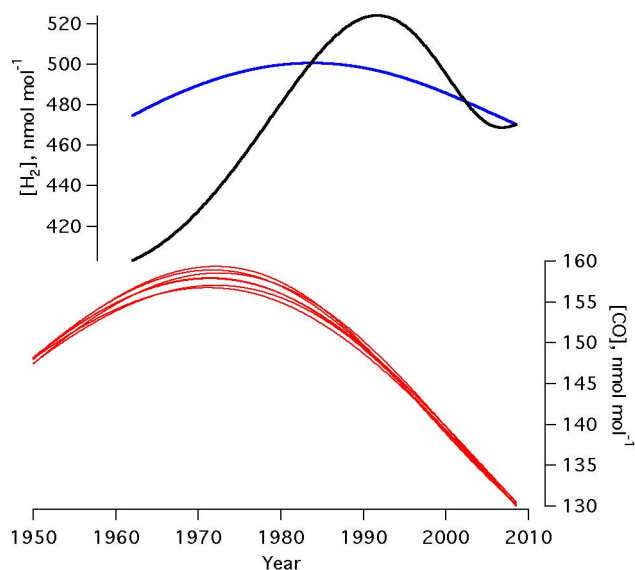
Fig. 9. [H_2] reconstructions from NEEM firn plotted together with [CO] reconstructions. Because the [H_2] reconstructions are only done to indicate an oldest-possible peak date for [H_2] over Greenland, fewer inversions were performed, and only with data from the NEEM EU borehole. The black line is an inversion based on the LGGE-GISPA model transfer function that provides the best fit to the data; the blue line is a corresponding inversion using the IN-STAAR model transfer function. As can be seen, [H_2] reconstructions are much more model-dependent than for [CO]. For comparison, the subset of successful [CO] scenarios reconstructed using only NEEM EU borehole data are shown in red.

to increase in the late 1980s (both in the Arctic and globally) while [CO] was not changing significantly.

The inferred later [H_2] peak as compared to [CO] (Fig. 9) is consistent with the hypothesis of [OH] increasing by a few percent from the early 1970s to the early 1980s while emissions are held constant. However, it may also be possible that the [CO]–[H_2] trend decoupling was driven by the introduction of catalytic converters starting in the 1970s. Catalytic converters reduce both CO and H_2 emissions, but they likely increase the overall H_2 / CO emission ratios from vehicles (Vollmer et al., 2010).

Because of their strongly connected sources and decoupled sinks, the H_2–CO pair may prove to be very useful in future studies of past atmospheric composition from ice cores and firn air. However, before quantitative information about past [H_2] can be obtained, a much better understanding of H_2 diffusion in firn and ice (including possible exchange between open and closed porosity in the lock-in zone) is needed.

5.6 Comparison with CO emission inventories

The RETRO emissions inventory (Schultz and Rast, 2007; Schultz et al., 2008) contains both anthropogenic and wild-

fire global gridded monthly CO emissions estimates back to 1960. The EDGAR-HYDE emissions inventory (van Aardenne et al., 2001) contains estimates of anthropogenic CO emissions by region back to 1890 AD, but provides only a single data point per decade. Figure 10 presents a comparison of CO emission estimates from these inventories with the reconstructed Greenland [CO] history.

The more recent ACCMIP inventory that was based on EDGAR-HYDE and RETRO for CO (Lamarque et al., 2010) suggests approximately factor of 2 lower combined anthropogenic and biomass-burning CO emissions in the 30–90° N latitude band in 1950 than in 2000. Lower atmospheric [CH_4] in 1950 (by $\approx 35\%$) (Etheridge et al., 1998) as well as ACCMIP-estimated lower anthropogenic NMHC emissions (factor of ≈ 2.5 lower) in the 30–90° N latitude band mean that the hydrocarbon oxidation source of CO was also lower in 1950 than in 2000. Assuming no large changes in the OH sink or biogenic NMHC emissions, the emissions inventories predict much lower [CO] in 1950 as compared to 2000. This is in stark contrast with the Greenland firn air [CO] reconstruction that shows $\approx 10\%$ higher [CO] in 1950 (≈ 140–150 nmol mol^{-1}) as compared to Arctic [CO] in 2000 from the NOAA flask network (≈ 130 nmol mol^{-1}).

Both EDGAR and RETRO also suggest that NH CO anthropogenic (and the combination of anthropogenic + wildfire) emissions continued to increase through the 1980s, although the RETRO estimates suggest that emissions in the 30–90° N latitude band leveled off (but did not decrease) after about 1980. As [CH_4] continued its rapid rise through the 1980s (≈ 15–20 nmol mol^{-1} a^{-1}) (Dlugokencky et al., 1994; Etheridge et al., 1998), the CH_4 oxidation source of CO continued to increase as well. This, again, appears inconsistent with our firn [CO] reconstruction, which shows Greenland [CO] peaking earlier between 1971 and 1983.

5.7 Information from a companion study of CO stable isotopes

Stable isotopes of CO can provide additional powerful clues for the interpretation of the changes in the CO budget over the period of our reconstruction. In a companion paper, Wang et al. (2012) presented measurements of $\delta^{13}CO$ and $\delta C^{18}O$ in firn air samples from the NEEM 2008 EU borehole, and used these measurements to reconstruct plausible CO isotopic histories. They found that the most likely atmospheric trend contained a small $\approx 1\,‰$ decrease in $\delta^{13}CO$ between 1950 and 2000, and a larger $\approx 2\,‰$ decrease in $\delta C^{18}O$ for the same time interval.

In addition, Wang et al. (2012) used a combination of atmospheric modeling and isotope mass balance to estimate the changing [CO] contributions from individual sources in the Arctic. They used the Arctic [CH_4] history (Buizert et al., 2012) and estimates of historical biomass and biofuel burning emissions (Ito and Penner, 2005) in combination with the MOZART-4 model to estimate the 1950–2000 [CO] at
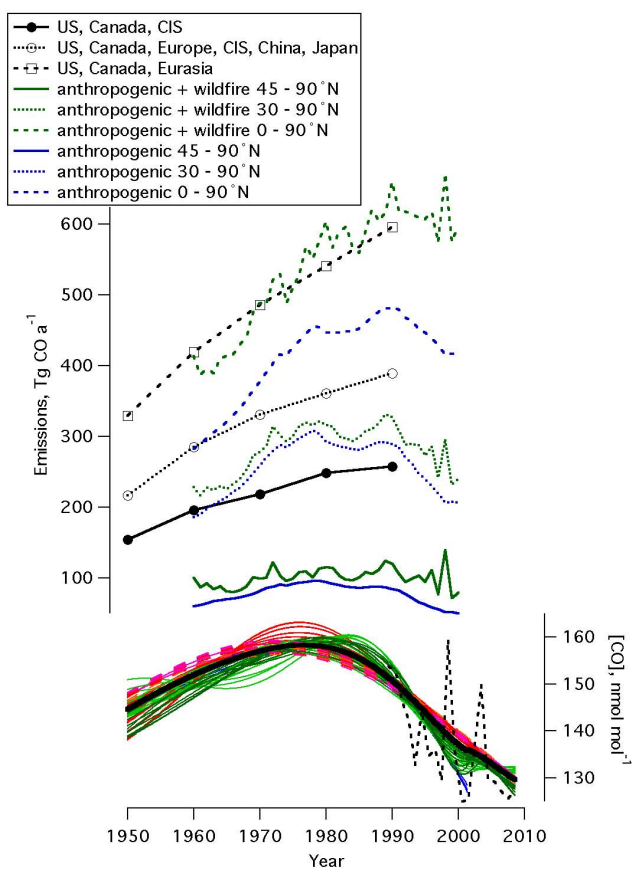
Fig. 10. A comparison of CO emissions from some available databases (upper part of plot) with the reconstructed [CO] historical scenarios over Greenland (lower part of plot; colors as in Fig. 8). EDGAR-HYDE estimates are in black. RETRO estimates are in blue and green. "CIS" denotes the former Soviet Union.

Iceland from these sources. Wang et al. (2012) then used an isotope mass balance model to derive the [CO] contributions from fossil fuel combustion and NMHC oxidation for the same period.

Their analysis found that fossil fuel combustion was likely the dominant contributor to Arctic [CO] during the entire 1950–2000 period. Contribution from CH_4 oxidation has the smallest uncertainties and was estimated to have increased from 18 to 29 nmol mol^{-1} [CO] during this period due to rising [CH_4]. No significant changes were inferred for the biomass burning contribution to [CO] (10–15 nmol mol^{-1}) during the entire period. The biofuel burning contribution likely increased from ≈ 10 nmol mol^{-1} in 1950 to ≈ 20 nmol mol^{-1} in 2000, with almost all of this increase taking place after 1970. The uncertainties in determined NMHC and fossil fuel combustion contributions were larger as they included additional uncertainties from firn air data and modeling. [CO] from NMHC oxidation was inferred to have been constant at 15–20 nmol mol^{-1} between 1950 and 1980, then decreased by 5–10 nmol mol^{-1} between 1980

and 2000, but with ≈ 15 nmol mol^{-1} error. [CO] from fossil fuel combustion was inferred (with a ≈ 20 nmol mol^{-1} error) to be relatively constant at 80–85 nmol mol^{-1} between 1950 and about 1975, then decreased dramatically by 25–30 nmol mol^{-1} between 1975 and 2000.

According to the Wang et al. (2012) CO isotopic analysis, the large ≈ 25 nmol mol^{-1} decrease in Arctic [CO] between the peak in the 1970s and 2000 is due almost entirely to reduced fossil fuel emissions, and they identify emission reductions from road transportation as the main cause.
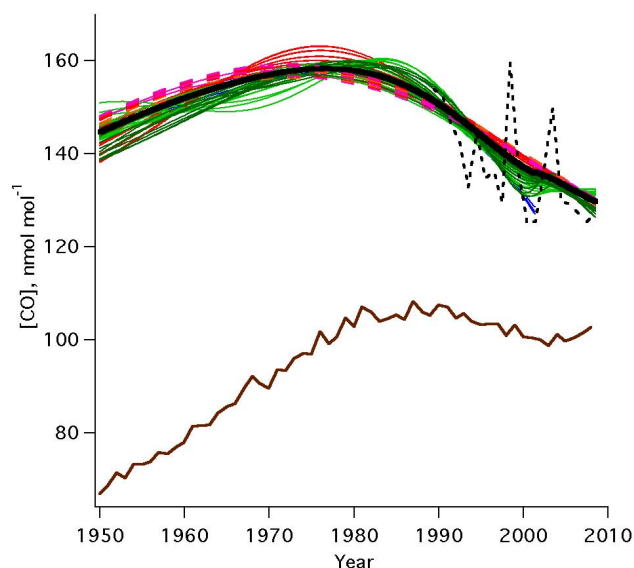
5.8 Comparison with CAM-Chem historical run

The same study that developed the ACCMIP inventory also used two chemistry-climate models to test this inventory by performing a historical run (Lamarque et al., 2010). We have obtained the historical [CO] output for the model grid points nearest NEEM from one of these models (CAM-Chem, (Lamarque et al., 2012)) and compare it to our firn-reconstructed [CO] in Fig. 11. The CAM-Chem run assumed constant biogenic NMHC emissions. CAM-Chem [CO] output for NEEM is consistent with the emissions inventories, predicting $\approx 40\%$ lower [CO] in 1950 than today, an emissions-driven broad [CO] peak around 1990, and only minimal reduction in [CO] from the peak to today's values. We note that CAM-Chem significantly underestimates NH high latitude [CO] during the last two decades (by $\sim 25\%$ for NEEM) when direct atmospheric monitoring was available; this result was already described (Lamarque et al., 2010).

Even with the CAM-Chem Arctic [CO] low bias taken into account, our firn-based Greenland [CO] reconstruction shows large disagreements with the CAM-Chem run. First, CAM-Chem appears to underestimate mean annual Arctic [CO] around 1950 by about a factor of 2. Second, the CAM-Chem historical run places the timing of the [CO] peak more than a decade later than predicted by our average scenario. Third, CAM-Chem underestimates the Arctic [CO] decline from peak values to today by a factor of ≈ 2.5.

5.9 Final interpretation of Greenland [CO] history

The combination of Greenland firn air results for CO stable isotopes and light alkanes, discussed above, argues strongly for CO fossil fuel emissions, and more specifically emissions from road transportation, being the main driver of the reconstructed [CO] trend over Greenland. Fossil fuel CO emissions appear to have remained relatively constant between 1950 and mid-1970s, and much of the modest ≈ 10 ppb increase in [CO] during this period was likely due to the rising CH_4 oxidation source. This result is surprising because fossil fuel combustion grew rapidly during this period (Schultz and Rast, 2007; Schultz et al., 2008; van Aardenne et al., 2001). We suggest that the explanation may be continuing improvements in combustion technology during the 1950–1970s period, which kept CO emissions relatively constant

Fig. 11. Comparison of atmospheric [CO] scenarios reconstructed from Greenland firn (colors as in Fig. 8) with results from the CAM historical run (brown). To approximate the NEEM surface mole fractions from CAM, [CO] values from the four closest grid points from CAM were averaged; these grid point coordinates form a box of 1.9° latitude × 2.5° longitude around NEEM. Annual means are plotted for CAM as calculated from the monthly [CO] output.

even as fossil fuel combustion by road transportation and other sources was increasing; this requires further investigation.

Fossil fuel CO emissions that affect the Arctic began to decline around the late 1970s, most likely driven by the regulation of CO emissions from transportation (via introduction of catalytic converters) in the United States and Western Europe starting in the 1970s (e.g., Bakwin et al., 1994; Granier et al., 2011; Kummer, 1980; Parrish, 2006). This reduced both the direct CO emissions as well as emissions of CO-precursor NMHCs.

Our reconstructed Greenland [CO] history is in conflict with existing CO emission inventories. When comparing the inventories with the [CO] history, it is important to take into account the effects of CO emission latitude and CO oxidation during transport to the Arctic. CO is a relatively short-lived gas, so shifting the average latitude of CO emissions to the south (due to falling emissions in Europe and North America, and growing emissions in India and Southeast Asia) would be expected to result in a CO decline over Greenland even if the overall emissions do not change.

This issue is addressed in our analysis via the inclusion of results from the CAM-Chem historical run (Fig. 11), which accounts for all these effects. From the CAM-Chem comparison to our reconstructed [CO] history, it is clear that latitudinal shifts in CO emissions cannot explain the surprisingly large discrepancy between reconstructed [CO] and emission inventories. If we assume no large changes in OH over time,

we must then conclude that the emission inventories contain large errors. First, CO emissions appear to be underestimated by as much as a factor of 2 for the period around 1950. Second, the inventories place the emission reductions (at least in the 30–90° N latitude band) too late by about a decade. Third, the CO emission reductions that have taken place in the last 2–3 decades appear to be underestimated in the inventories by as much as a factor of 2.5. These errors are a serious concern, as these existing inventories are being used for the Coupled Model Intercomparison Project Phase 5 (CMIP5) for the IPCC 5th Assessment Report (Lamarque et al., 2010).

Unfortunately, neither the [CO]–d[CH$_4$]/dt comparison nor the [CO]–[H$_2$] comparison are able to provide conclusive evidence about the role of possible OH changes in the [CO] history. Both of these comparisons (Sects. 5.2 and 5.5) are consistent with the hypothesis of changes in OH playing a significant role in the reconstructed histories of all considered trace gases. For example, an increase in OH of ≈ 5 % between 1975 and 1985 could explain the reconstructed [CO] trend during this period if CO emissions are held constant; this trend could also be consistent with reconstructed [H$_2$] and d[CH$_4$]/dt, if CH$_4$ sources are allowed to continue increasing during this period.

One possibility is that increased emissions of nitrogen oxides (NO$_x$) may have resulted in modest OH growth between 1950 and 1985 because NO$_x$ promotes OH recycling in the troposphere (e.g., Brasseur et al., 1999). The EDGAR-HYDE emissions inventory indicates increasing NO$_x$ emissions from the NH midlatitude regions between 1950 and 1990 (van Aardenne et al., 2001), and the RETRO emissions inventory also indicates increasing NO$_x$ emissions between 1960 and 1980 in the 30–90° N latitude band (Schultz and Rast, 2007; Schultz et al., 2008). Such an explanation would allow to partially reconcile the CO emission inventories with our [CO] reconstruction. However, it also appears entirely possible to explain the [CO], [H$_2$] and d[CH$_4$]/dt trends using scenarios with constant OH and varying emissions. Based on the comprehensive Montzka et al. (2011) study discussed in Sect. 5.4, we consider it unlikely that changes in OH were the main driver of the reconstructed [CO] trend.

6 Summary and conclusions

We have presented the first firn air record of past atmospheric [CO] for the NH high latitudes, covering the period from 1950 to 2008. The good agreement among [CO] records from three different firn air sites (NEEM, NGRIP and Summit) confirms that CO is well preserved in the firn at inland Greenland sites. The quality of the firn air records is further confirmed by the good agreement with direct atmospheric measurements of [CO] in the Arctic, which began in 1980. Peak-shaped atmospheric trends are challenging to reconstruct from firn air data due to the smoothing effect of molecular diffusion. A new methodology for this reconstruction

has been developed and its robustness tested. Different firn gas transport models, combinations of firn air sites and optimal solution definitions lead to consistent results for [CO] peak height and constrain the [CO] peak date with $\approx \pm 6$ year uncertainty. The recent part of the reconstructed trend is consistent with available atmospheric data.

Our [CO] reconstruction shows relatively high values of ≈ 140–$150\,\mathrm{nmol\,mol^{-1}}$ in 1950, which is higher than Arctic [CO] in the last decade ($\approx 130\,\mathrm{nmol\,mol^{-1}}$); [CO] then increased slightly by ≈ 10–$15\,\mathrm{nmol\,mol^{-1}}$ to a peak in the late 1970s, and then decreased strongly by $\approx 30\,\mathrm{nmol\,mol^{-1}}$ to values observed in the last decade. We interpret the Arctic [CO] trend to be driven mainly by fossil fuel emissions, with relatively constant emissions in the 1950–1970s period, when the effect of increasing fossil fuel combustion may have been offset by continuing improvements in combustion technology. The [CO] decline in the 1980s and 1990s was likely driven by decreasing emissions from road transportation due to the introduction of catalytic converters in North America and Europe.

Our results are in strong disagreement with the results of a CTM historical run that used available CO emissions inventories, which predict 1950 Arctic [CO] to be $\approx 40\,\%$ lower than today, a very large [CO] increase of $\approx 60\,\%$ from 1950 to peak values, a later Arctic [CO] peak around 1990, and only a small $< 10\,\mathrm{nmol\,mol^{-1}}$ [CO] decrease from peak values to today. We suggest that this disagreement results mainly from large errors in the available CO emission inventories.

Several robust new data sets of reactive trace gas atmospheric histories are now available from Greenland firn, including [CO] (this study), CO stable isotopes (Wang et al., 2012) and light non-methane hydrocarbon mole fractions (Aydin et al., 2011, Worton et al., 2012; Helmig et al., 2013). We suggest that much more can now be learned about changes in Northern Hemisphere emissions as well as possibly in atmospheric chemistry during the 1950–2000 time period by doing iterative, long historical CTM runs that use these new data as constraints, and we hope that the atmospheric modeling community will undertake such a study.

Supplementary material related to this article is available online at: http://www.atmos-chem-phys.net/13/7567/2013/acp-13-7567-2013-supplement.pdf.

References

Assonov, S. S., Brenninkmeijer, C. A. M., Jöckel, P., Mulvaney, R., Bernard, S., and Chappellaz, J.: Evidence for a CO increase in the SH during the 20th century based on firn air samples from Berkner Island, Antarctica, Atmos. Chem. Phys., 7, 295–308, doi:10.5194/acp-7-295-2007, 2007.

Aydin, M., Verhulst, K. R., Saltzman, E. S., Battle, M. O., Montzka, S. A., Blake, D. R., Tang, Q., and Prather, M. J.: Recent decreases in fossil-fuel emissions of ethane and methane derived from firn air, Nature, 476, 198–201, 2011.

Bakwin, P. S., Tans, P. P., and Novelli, P. C.: Carbon-Monoxide Budget in the Northern Hemisphere, Geophys. Res. Lett., 21, 433–436, 1994.

Battle, M., Bender, M., Sowers, T., Tans, P. P., Butler, J. H., Elkins, J. W., Ellis, J. T., Conway, T., Zhang, N., Lang, P., and Clarke, A. D.: Atmospheric gas concentrations over the past century measured in air from firn at the South Pole, Nature, 383, 231–235, 1996.

Bernard, S., Röckmann, T., Kaiser, J., Barnola, J.-M., Fischer, H., Blunier, T., and Chappellaz, J.: Constraints on N$_2$O budget changes since pre-industrial time from new firn air and ice core isotope measurements, Atmos. Chem. Phys., 6, 493–503, doi:10.5194/acp-6-493-2006, 2006.

Bousquet, P., Hauglustaine, D. A., Peylin, P., Carouge, C., and Ciais, P.: Two decades of OH variability as inferred by an inversion of atmospheric transport and chemistry of methyl chloroform, Atmos. Chem. Phys., 5, 2635–2656, doi:10.5194/acp-5-2635-2005, 2005.

Brasseur, G., Orlando, J., and Tyndall, G.: Atmospheric Chemistry and Global Change, in: Topics in Environmental Chemistry, edited by: Birks, J., Oxford University Press, New York, 654 pp., 1999.

Buizert, C., Martinerie, P., Petrenko, V. V., Severinghaus, J. P., Trudinger, C. M., Witrant, E., Rosen, J. L., Orsi, A. J., Rubino, M., Etheridge, D. M., Steele, L. P., Hogan, C., Laube, J. C., Sturges, W. T., Levchenko, V. A., Smith, A. M., Levin, I., Conway, T. J., Dlugokencky, E. J., Lang, P. M., Kawamura, K., Jenk, T. M., White, J. W. C., Sowers, T., Schwander, J., and Blunier, T.: Gas transport in firn: multiple-tracer characterisation and model intercomparison for NEEM, Northern Greenland, Atmos. Chem. Phys., 12, 4259–4277, doi:10.5194/acp-12-4259-2012, 2012.

Clark, I. D., Henderson, L., Chappellaz, J., Fisher, D., Koerner, R., Worthy, D. E. J., Kotzer, T., Norman, A. L., and Barnola, J. M.: CO_2 isotopes as tracers of firn air diffusion and age in an Arctic ice cap with summer melting, Devon Island, Canada, J. Geophys. Res.-Atmos., 112, D01301, doi:10.1029/2006JD007471, 2007.

Crutzen, P.: Discussion of Chemistry of Some Minor Constituents in Stratosphere and Troposphere, Pure Appl. Geophys., 106, 1385–1399, 1973.

Crutzen, P. J. and Brühl, C.: A Model Study of Atmospheric Temperatures and the Concentrations of Ozone, Hydroxyl, and Some Other Photochemically Active Gases During the Glacial, the Preindustrial Holocene and the Present, Geophys. Res. Lett., 20, 1047–1050, 1993.

Daniel, J. S. and Solomon, S.: On the climate forcing of carbon monoxide, J. Geophys. Res.-Atmos., 103, 13249–13260, 1998.

Dentener, F., Peters, W., Krol, M., van Weele, M., Bergamaschi, P., and Lelieveld, J.: Interannual variability and trend of CH_4 lifetime as a measure for OH changes in the 1979–1993 time period, J. Geophys. Res.-Atmos., 108, 4442, doi:10.1029/2002JD002916, 2003.

Dlugokencky, E. J., Steele, L. P., Lang, P. M., and Masarie, K. A.: The Growth Rate and Distribution of Atmospheric Methane, J. Geophys. Res.-Atmos., 99, 17021–17043, 1994.

Dlugokencky, E. J., Houweling, S., Bruhwiler, L., Masarie, K. A., Lang, P. M., Miller, J. B., and Tans, P. P.: Atmospheric methane levels off: Temporary pause or a new steady-state?, Geophys. Res. Lett., 30, 1992, doi:10.1029/2003GL018126, 2003.

Duncan, B. N., Logan, J. A., Bey, I., Megretskaia, I. A., Yantosca, R. M., Novelli, P. C., Jones, N. B., and Rinsland, C. P.: Global budget of CO, 1988–1997: Source estimates and validation with a global model, J. Geophys. Res.-Atmos., 112, D22301, doi:10.1029/2007JD008459, 2007.

Etheridge, D. M., Steele, L. P., Francey, R. J., and Langenfelds, R. L.: Atmospheric methane between 1000 AD and present: Evidence of anthropogenic emissions and climatic variability, J. Geophys. Res.-Atmos., 103, 15979–15993, 1998.

Ferretti, D. F., Miller, J. B., White, J. W. C., Etheridge, D. M., Lassey, K. R., Lowe, D. C., Meure, C. M. M., Dreier, M. F., Trudinger, C. M., van Ommen, T. D., and Langenfelds, R. L.: Unexpected changes to the global methane budget over the past 2000 years, Science, 309, 1714–1717, 2005.

Forster, G., Sturges, W. T., Fleming, Z. L., Bandy, B. J., and Emeis, S.: A year of H_2 measurements at Weybourne Atmospheric Observatory, UK, Tellus B, 64, 17771, doi:10.3402/tellusb.v64i0.17771, 2012.

Francey, R. J., Steele, L. P., Spencer, D. A., Langenfelds, R. L., Law, R. M., Krummel, P. B., Fraser, P. J., Etheridge, D. M., Derek, N., Coram, S. A., Cooper, L. N., Allison, C. E., Porter, L., and Baly, S.: The CSIRO (Australia) measurement of greenhouse gases in the global atmosphere, in: Baseline Atmospheric Program Australia, edited by: Tindale, N. W., Derek, N., and Fraser, P. J., Melbourne, Bureau of Meteorology and CSIRO Atmospheric Research, 42–53, 2003.

Granier, C., Bessagnet, B., Bond, T., D'Angiola, A., van der Gon, H. D., Frost, G. J., Heil, A., Kaiser, J. W., Kinne, S., Klimont, Z., Kloster, S., Lamarque, J. F., Liousse, C., Masui, T., Meleux, F., Mieville, A., Ohara, T., Raut, J. C., Riahi, K., Schultz, M. G., Smith, S. J., Thompson, A., van Aardenne, J., van der Werf, G. R., and van Vuuren, D. P.: Evolution of anthropogenic and biomass burning emissions of air pollutants at global and regional scales during the 1980–2010 period, Climatic Change, 109, 163–190, 2011.

Haan, D. and Raynaud, D.: Ice core record of CO variations during the last two millennia: atmospheric implications and chemical interactions within the Greenland ice, Tellus B, 50, 253–262, 1998.

Haan, D., Martinerie, P., and Raynaud, D.: Ice core data of atmospheric carbon monoxide over Antarctica and Greenland during the last 200 years, Geophys. Res. Lett., 23, 2235–2238, 1996.

Hammer, S. and Levin, I.: Seasonal variation of the molecular hydrogen uptake by soils inferred from continuous atmospheric observations in Heidelberg, southwest Germany, Tellus B, 61, 556–565, 2009.

Helmig, D., Bottenheim, J. W., Galbally, I. E., Lewis, A., Milton, M. J. T., Penkett, S., Plass-Duelmer, C., Reimann, S., Tans, P., and Thiel, S.: Volatile Organic Compounds in the Global Atmosphere, Eos Trans. AGU, 90, 513–514, 2009.

Helmig, D., Petrenko, V., Martinerie, P., Witrant, E., Röckmann, T., Zuiderweg, A., Holzinger, R., Hueber, J., Stephens, C., White, J., Sturges, W., Baker, A., Blunier, T., Etheridge, D., Rubino, M., and Tans, P.: Reconstruction of Northern Hemisphere 1950–2010 atmospheric non-methane hydrocarbons, Atmos. Chem. Phys. Discuss., 13, 12991–13043, doi:10.5194/acpd-13-12991-2013, 2013.

Ito, A. and Penner, J. E.: Historical emissions of carbonaceous aerosols from biomass and fossil fuel burning for the period 1870–2000, Global Biogeochem. Cy., 19, GB2028, doi:10.1029/2004GB002374, 2005.

Jordan, A. and Steinberg, B.: Calibration of atmospheric hydrogen measurements, Atmos. Meas. Tech., 4, 509–521, doi:10.5194/amt-4-509-2011, 2011.

Khalil, M. A. K. and Rasmussen, R. A.: Carbon Monoxide in the Earth's Atmosphere–Increasing Trend, Science, 224, 54–56, 1984.

Khalil, M. A. K. and Rasmussen, R. A.: Carbon Monoxide in the Earth's Atmosphere–Indications of a Global Increase, Nature, 332, 242–245, 1988.

Khalil, M. A. K. and Rasmussen, R. A.: Global Increase of Atmospheric Molecular-Hydrogen, Nature, 347, 743–745, 1990.

Khalil, M. A. K. and Rasmussen, R. A.: Global Decrease in Atmospheric Carbon Monoxide Concentration, Nature, 370, 639–641, 1994.

Krol, M. and Lelieveld, J.: Can the variability in tropospheric OH be deduced from measurements of 1,1,1-trichloroethane (methyl chloroform)?, J. Geophys. Res.-Atmos., 108, 4125, doi:10.1029/2002JD002423, 2003.

Kummer, J. T.: Catalysts for Automobile Emission Control, Prog. Energ. Combust., 6, 177–199, 1980.

Lamarque, J.-F., Bond, T. C., Eyring, V., Granier, C., Heil, A., Klimont, Z., Lee, D., Liousse, C., Mieville, A., Owen, B.,

Schultz, M. G., Shindell, D., Smith, S. J., Stehfest, E., Van Aardenne, J., Cooper, O. R., Kainuma, M., Mahowald, N., McConnell, J. R., Naik, V., Riahi, K., and van Vuuren, D. P.: Historical (1850–2000) gridded anthropogenic and biomass burning emissions of reactive gases and aerosols: methodology and application, Atmos. Chem. Phys., 10, 7017–7039, doi:10.5194/acp-10-7017-2010, 2010.

Lamarque, J.-F., Emmons, L. K., Hess, P. G., Kinnison, D. E., Tilmes, S., Vitt, F., Heald, C. L., Holland, E. A., Lauritzen, P. H., Neu, J., Orlando, J. J., Rasch, P. J., and Tyndall, G. K.: CAM-chem: description and evaluation of interactive atmospheric chemistry in the Community Earth System Model, Geosci. Model Dev., 5, 369–411, doi:10.5194/gmd-5-369-2012, 2012.

Ljung, L.: System Identification: Theory for the User, Information and System Sciences, PTR Prentice Hall, Upper Saddle River, NJ, 2nd Edn., 1999.

MacFarling Meure, C.: The Variation of Atmospheric Carbon Dioxide, Methane and Nitrous Oxide During the Holocene from Ice Core Analysis, Ph.D. thesis, The University of Melbourne, 2004.

Martinerie, P., Brasseur, G. P., and Granier, C.: The Chemical Composition of Ancient Atmospheres – a Model Study Constrained by Ice Core Data, J. Geophys. Res.-Atmos., 100, 14291–14304, 1995.

Masarie, K. A., Langenfelds, R. L., Allison, C. E., Conway, T. J., Dlugokencky, E. J., Francey, R. J., Novelli, P. C., Steele, L. P., Tans, P. P., Vaughn, B., and White, J. W. C.: NOAA/CSIRO Flask Air Intercomparison Experiment: A strategy for directly assessing consistency among atmospheric measurements made by independent laboratories, J. Geophys. Res.-Atmos., 106, 20445–20464, 2001.

Mikaloff-Fletcher, S. E. M., Tans, P. P., Bruhwiler, L. M., Miller, J. B., and Heimann, M.: CH_4 sources estimated from atmospheric observations of CH_4 and its $^{13}C/^{12}C$ isotopic ratios: 1. Inverse modeling of source processes, Global Biogeochem. Cy., 18. GB4004, doi:10.1029/2004GB002223, 2004.

Montzka, S. A., Krol, M., Dlugokencky, E., Hall, B., Jockel, P., and Lelieveld, J.: Small Interannual Variability of Global Atmospheric Hydroxyl, Science, 331, 67–69, 2011

Novelli, P. C., Steele, L. P., and Tans, P. P.: Mixing Ratios of Carbon Monoxide in the Troposphere, J. Geophys. Res.-Atmos., 97, 20731–20750, 1992.

Novelli, P. C., Masarie, K. A., Tans, P. P., and Lang, P. M.: Recent Changes in Atmospheric Carbon Monoxide, Science, 263, 1587–1590, 1994.

Novelli, P. C., Connors, V. S., Reichle, H. G., Anderson, B. E., Brenninkmeijer, C. A. M., Brunke, E. G., Doddridge, B. G., Kirchhoff, V. W. J. H., Lam, K. S., Masarie, K. A., Matsuo, T., Parrish, D. D., Scheel, H. E., and Steele, L. P.: An internally consistent set of globally distributed atmospheric carbon monoxide mixing ratios developed using results from an intercomparison of measurements, J. Geophys. Res.-Atmos., 103, 19285–19293, 1998a.

Novelli, P. C., Masarie, K. A., and Lang, P. M.: Distributions and recent changes of carbon monoxide in the lower troposphere, J. Geophys. Res.-Atmos., 103, 19015–19033, 1998b.

Novelli, P. C., Lang, P. M., Masarie, K. A., Hurst, D. F., Myers, R., and Elkins, J. W.: Molecular hydrogen in the troposphere: Global distribution and budget, J. Geophys. Res.-Atmos., 104, 30427–30444, 1999.

Novelli, P. C., Masarie, K. A., Lang, P. M., Hall, B. D., Myers, R. C., and Elkins, J. W.: Reanalysis of tropospheric CO trends: Effects of the 1997–1998 wildfires, J. Geophys. Res.-Atmos., 108, 4464, doi:10.1029/2002JD003031, 2003.

Novelli, P. C., Crotwell, A. M., and Hall, B. D.: Application of Gas Chromatography with a Pulsed Discharge Helium Ionization Detector for Measurements of Molecular Hydrogen in the Atmosphere, Environ. Sci. Tech., 43, 2431–2436, 2009.

Parrish, D. D.: Critical evaluation of US on-road vehicle emission inventories, Atmos. Environ., 40, 2288–2300, 2006.

Pozzer, A., Pollmann, J., Taraborrelli, D., Jöckel, P., Helmig, D., Tans, P., Hueber, J., and Lelieveld, J.: Observed and simulated global distribution and budget of atmospheric C_2-C_5 alkanes, Atmos. Chem. Phys., 10, 4403–4422, doi:10.5194/acp-10-4403-2010, 2010.

Price, H., Jaegle, L., Rice, A., Quay, P., Novelli, P. C., and Gammon, R.: Global budget of molecular hydrogen and its deuterium content: Constraints from ground station, cruise, and aircraft observations, J. Geophys. Res.-Atmos., 112, D22108, doi:10.1029/2006JD008152, 2007.

Prinn, R., Cunnold, D., Simmonds, P., Alyea, F., Boldi, R., Crawford, A., Fraser, P., Gutzler, D., Hartley, D., Rosen, R., and Rasmussen, R.: Global Average Concentration and Trend for Hydroxyl Radicals Deduced from ALE/GAGE Trichloroethane (Methyl Chloroform) Data for 1978–1990, J. Geophys. Res.-Atmos., 97, 2445–2461, 1992.

Prinn, R. G., Weiss, R. F., Miller, B. R., Huang, J., Alyea, F. N., Cunnold, D. M., Fraser, P. J., Hartley, D. E., and Simmonds, P. G.: Atmospheric Trends and Lifetime of CH_3CCl_3 and Global OH Concentrations, Science, 269, 187–192, 1995.

Prinn, R. G., Huang, J., Weiss, R. F., Cunnold, D. M., Fraser, P. J., Simmonds, P. G., McCulloch, A., Harth, C., Salameh, P., O'Doherty, S., Wang, R. H. J., Porter, L., and Miller, B. R.: Evidence for substantial variations of atmospheric hydroxyl radicals in the past two decades, Science, 292, 1882–1888, 2001.

Prinn, R. G., Huang, J., Weiss, R. F., Cunnold, D. M., Fraser, P. J., Simmonds, P. G., McCulloch, A., Harth, C., Reimann, S., Salameh, P., O'Doherty, S., Wang, R. H. J., Porter, L. W., Miller, B. R., and Krummel, P. B.: Evidence for variability of atmospheric hydroxyl radicals over the past quarter century, Geophys. Res. Lett., 32, L07809, doi:10.1029/2004GL022228, 2005.

Rinsland, C. P. and Levine, J. S.: Free Tropospheric Carbon Monoxide Concentrations in 1950 and 1951 Deduced from Infrared Total Column Amount Measurements, Nature, 318, 250–254, 1985.

Rommelaere, V., Arnaud, L., and Barnola, J. M.: Reconstructing recent atmospheric trace gas concentrations from polar firn and bubbly ice data by inverse methods, J. Geophys. Res.-Atmos., 102, 30069–30083, 1997.

Sapart, C. J., Martinerie, P., Witrant, E., Chappellaz, J., van de Wal, R. S. W., Sperlich, P., van der Veen, C., Bernard, S., Sturges, W. T., Blunier, T., Schwander, J., Etheridge, D., and Röckmann, T.: Can the carbon isotopic composition of methane be reconstructed from multi-site firn air measurements?, Atmos. Chem. Phys., 13, 6993–7005, doi:10.5194/acp-13-6993-2013, 2013.

Schultz, M. and Rast, S.: RETRO emission datasets and methodologies, RETRO Report D1-6, 144 pp., 2007.

Schultz, M. G., Heil, A., Hoelzemann, J. J., Spessa, A., Thonicke, K., Goldammer, J. G., Held, A. C., Pereira, J. M. C., and van het Bolscher, M.: Global wildland fire emissions

from 1960 to 2000, Global Biogeochem. Cy., 22, GB2002, doi:10.1029/2007GB003031, 2008.

Schwander, J., Barnola, J. M., Andrie, C., Leuenberger, M., Ludin, A., Raynaud, D., and Stauffer, B.: The Age of the Air in the Firn and the Ice at Summit, Greenland, J. Geophys. Res.-Atmos., 98, 2831–2838, 1993.

Severinghaus, J. P. and Battle, M. O.: Fractionation of gases in polar ice during bubble close-off: New constraints from firn air Ne, Kr and Xe observations, Earth Planet. Sci. Lett., 244, 474–500, 2006.

Shindell, D. T., Faluvegi, G., Stevenson, D. S., Krol, M. C., Emmons, L. K., Lamarque, J. F., Petron, G., Dentener, F. J., Ellingsen, K., Schultz, M. G., Wild, O., Amann, M., Atherton, C. S., Bergmann, D. J., Bey, I., Butler, T., Cofala, J., Collins, W. J., Derwent, R. G., Doherty, R. M., Drevet, J., Eskes, H. J., Fiore, A. M., Gauss, M., Hauglustaine, D. A., Horowitz, L. W., Isaksen, I. S. A., Lawrence, M. G., Montanaro, V., Muller, J. F., Pitari, G., Prather, M. J., Pyle, J. A., Rast, S., Rodriguez, J. M., Sanderson, M. G., Savage, N. H., Strahan, S. E., Sudo, K., Szopa, S., Unger, N., van Noije, T. P. C., and Zeng, G.: Multimodel simulations of carbon monoxide: Comparison with observations and projected near-future changes, J. Geophys. Res.-Atmos., 111, D19306, doi:10.1029/2006JD007100, 2006.

Simpson, I. J., Akagi, S. K., Barletta, B., Blake, N. J., Choi, Y., Diskin, G. S., Fried, A., Fuelberg, H. E., Meinardi, S., Rowland, F. S., Vay, S. A., Weinheimer, A. J., Wennberg, P. O., Wiebring, P., Wisthaler, A., Yang, M., Yokelson, R. J., and Blake, D. R.: Boreal forest fire emissions in fresh Canadian smoke plumes: C1-C10 volatile organic compounds (VOCs), CO_2, CO, NO_2, NO, HCN and CH_3CN, Atmos. Chem. Phys., 11, 6445–6463, doi:10.5194/acp-11-6445-2011, 2011.

Sowers, T., Bernard, S., Aballain, O., Chappellaz, J., Barnola, J. M., and Marik, T.: Records of the delta C-13 of atmospheric CH_4 over the last 2 centuries as recorded in Antarctic snow and ice, Global Biogeochem. Cy., 19, GB2002, doi:10.1029/2004GB002408, 2005.

Spivakovsky, C. M., Logan, J. A., Montzka, S. A., Blakanski, Y. J., Foreman-Fowler, M., Jones, D. B. A., Horowitz, L. W., Fusco, A. C., Brenninkmeijer, C. A. M., Prather, M. J., Wofsy, S. C., and McElroy, M. B.: Three-dimensional climatological distribution of tropospheric OH: update and evaluation, J. Geophys. Res.-Atmos., 105, 8931–8980, 2000.

Thompson, A. M.: The Oxidizing Capacity of the Earths Atmosphere–Probable Past and Future Changes, Science, 256, 1157–1165, 1992.

Thompson, A. M., Chappellaz, J. A., Fung, I. Y., and Kucsera, T. L.: The Atmospheric CH_4 Increase since the Last Glacial Maximum. 2. Interactions with Oxidants, Tellus B, 45, 242–257, 1993.

Trudinger, C. A., Etheridge, D. M., Rayner, P. J., Enting, I. G., Sturrock, G. A., and Langenfelds, R. L.: Reconstructing atmospheric histories from measurements of air composition in firn, J. Geophys. Res., 107, 4780, doi:10.1029/2002JD002545, 2002.

Trudinger, C. M., Enting, I. G., Etheridge, D. M., Francey, R. J., Levchenko, V. A., Steele, L. P., Raynaud, D., and Arnaud, L.: Modeling air movement and bubble trapping in firn, J. Geophys. Res.-Atmos., 102, 6747–6763, 1997.

van Aardenne, J. A., Dentener, F. J., Olivier, J. G. J., Goldewijk, C. G. M. K., and Lelieveld, J.: A 1° × 1° resolution data set of historical anthropogenic trace gas emissions for the period 1890–1990, Global Biogeochem. Cy., 15, 909–928, 2001.

van der Werf, G. R., Randerson, J. T., Giglio, L., Collatz, G. J., Kasibhatla, P. S., and Arellano Jr., A. F.: Interannual variability in global biomass burning emissions from 1997 to 2004, Atmos. Chem. Phys., 6, 3423–3441, doi:10.5194/acp-6-3423-2006, 2006.

Vollmer, M. K., Walter, S., Bond, S. W., Soltic, P., and Röckmann, T.: Molecular hydrogen (H_2) emissions and their isotopic signatures (H/D) from a motor vehicle: implications on atmospheric H_2, Atmos. Chem. Phys., 10, 5707–5718, doi:10.5194/acp-10-5707-2010, 2010.

Wang, Z. and Mak, J. E.: A new CF-IRMS system for quantifying stable isotopes of carbon monoxide from ice cores and small air samples, Atmos. Meas. Tech., 3, 1307–1317, doi:10.5194/amt-3-1307-2010, 2010.

Wang, Z., Chappellaz, J., Park, K., and Mak, J. E.: Large Variations in Southern Hemisphere Biomass Burning During the Last 650 Years, Science, 330, 1663–1666, 2010.

Wang, Z., Chappellaz, J., Martinerie, P., Park, K., Petrenko, V., Witrant, E., Emmons, L. K., Blunier, T., Brenninkmeijer, C. A. M., and Mak, J. E.: The isotopic record of Northern Hemisphere atmospheric carbon monoxide since 1950: implications for the CO budget, Atmos. Chem. Phys., 12, 4365–4377, doi:10.5194/acp-12-4365-2012, 2012.

Witrant, E. and Martinerie, P.: "Input Estimation from Sparse Measurements in LPV Systems and Isotopic Ratios in Polar Firns", Proc. of the 5th IFAC Symposium on System Structure and Control, 659–664, doi:10.3182/20130204-3-FR-2033.00201, 2013.

Witrant, E., Martinerie, P., Hogan, C., Laube, J. C., Kawamura, K., Capron, E., Montzka, S. A., Dlugokencky, E. J., Etheridge, D., Blunier, T., and Sturges, W. T.: A new multi-gas constrained model of trace gas non-homogeneous transport in firn: evaluation and behaviour at eleven polar sites, Atmos. Chem. Phys., 12, 11465–11483, doi:10.5194/acp-12-11465-2012, 2012.

Worton, D. R., Sturges, W. T., Reeves, C. E., Newland, M. J., Penkett, S., Atlas, E., Stroud, V., Johnson, K., Schmidbauer, N., Solberg, S., Schwander, J., and Barnola, J. M.: Evidence from firn air for recent decreases in non-methane hydrocarbons and a 20th century increase in nitrogen oxides in the northern hemisphere, Atmos. Environ., 54, 592–602, 2012.

Xiao, Y. P., Logan, J. A., Jacob, D. J., Hudman, R. C., Yantosca, R., and Blake, D. R.: Global budget of ethane and regional constraints on US sources, J. Geophys. Res.-Atmos., 113, D21306, doi:10.1029/2007JD009415, 2008.

Yurganov, L. N., Grechko, E. I., and Dzhola, A. V.: Zvenigorod carbon monoxide total column time series: 27 yr of measurements, Chemosphere, 1, 127–136, 1999.